

JGR Biogeosciences

RESEARCH ARTICLE

10.1029/2022JG007188

Key Points:

- Dissolved organic matter (DOM) in surface streams was younger in carbon age than in outflows, despite similarity in molecular composition
- Regionally, DOM aromaticity increased with older carbon ages, due to lower relative contributions of modern, aliphatic-rich DOM to runoff
- Trends between water isotopes and DOM composition suggest that atmospheric deposition may be a control on outflow DOM composition

Supporting Information:

Supporting Information may be found in the online version of this article.

Correspondence to:

A. D. Holt,
adh19d@fsu.edu

Citation:

Holt, A. D., Kellerman, A. M., Battin, T. I., McKenna, A. M., Hood, E., Andino, P., et al. (2023). A tropical cocktail of organic matter sources: Variability in supraglacial and glacier outflow dissolved organic matter composition and age across the Ecuadorian Andes. *Journal of Geophysical Research: Biogeosciences*, 128, e2022JG007188. <https://doi.org/10.1029/2022JG007188>

Received 21 SEP 2022

Accepted 2 MAY 2023

Author Contributions:

Conceptualization: Amy D. Holt, Tom. I. Battin, Robert G. M. Spencer

Data curation: Amy D. Holt, Amy M. McKenna, Hannes Peter

Formal analysis: Amy D. Holt











Funding acquisition: Tom. I. Battin, Eran Hood, Robert G. M. Spencer

Investigation: Amy D. Holt, Anne M. Kellerman, Amy M. McKenna, Patricio Andino, Verónica Crespo-Pérez, Martina Schön, Vincent De Staercke, Michail Styllas, Matteo Tolosano

Project Administration: Amy D. Holt, Tom. I. Battin, Robert G. M. Spencer

Resources: Tom. I. Battin, Patricio Andino, Verónica Crespo-Pérez, Robert G. M. Spencer

A Tropical Cocktail of Organic Matter Sources: Variability in Supraglacial and Glacier Outflow Dissolved Organic Matter Composition and Age Across the Ecuadorian Andes

Amy D. Holt¹ , Anne M. Kellerman¹ , Tom. I. Battin² , Amy M. McKenna³ , Eran Hood⁴ , Patricio Andino⁵, Verónica Crespo-Pérez⁵ , Hannes Peter² , Martina Schön² , Vincent De Staercke², Michail Styllas² , Matteo Tolosano², and Robert G. M. Spencer¹ 

¹National High Magnetic Field Laboratory Geochemistry Group, Department of Earth, Ocean, and Atmospheric Science, Florida State University, Tallahassee, FL, USA, ²River Ecology Laboratory, Ecole Polytechnique Fédérale de Lausanne, Lausanne, Switzerland, ³Department of Soil Crop Sciences, Colorado State University, Fort Collins, CO, USA, ⁴Program on the Environment and Alaska Coastal Rainforest Center, University of Alaska Southeast, Juneau, AK, USA, ⁵Laboratorio de Limnología, Museo de Zoología QCAZ I, Escuela de Ciencias Biológicas, Pontificia Universidad Católica del Ecuador, Quito, Ecuador

Abstract The biogeochemistry of rapidly retreating Andean glaciers is poorly understood, and Ecuadorian glacier dissolved organic matter (DOM) composition is unknown. This study examined molecular composition and carbon isotopes of DOM from supraglacial and outflow streams ($n = 5$ and 14 , respectively) across five ice capped volcanoes in Ecuador. Compositional metrics were paired with streamwater isotope analyses ($\delta^{18}\text{O}$) to assess if outflow DOM composition was associated with regional precipitation gradients and thus an atmospheric origin of glacier DOM. Ecuadorian glacier outflows exported ancient, biolabile dissolved organic carbon (DOC), and DOM contained a high relative abundance (RA) of aliphatic and peptide-like compounds ($\geq 27\%$ RA). Outflows were consistently more depleted in $\Delta^{14}\text{C}$ -DOC (i.e., older) compared to supraglacial streams (mean -195.2 and -61.3% respectively), perhaps due to integration of spatially heterogeneous and variably aged DOM pools across the supraglacial environment, or incorporation of aged subglacial OM as runoff was routed to the outflow. Across Ecuador, $\Delta^{14}\text{C}$ -DOC enrichment was associated with decreased aromaticity of DOM, due to increased contributions of organic matter (OM) from microbial processes or atmospheric deposition of recently fixed and subsequently degraded OM (e.g., biomass burning byproducts). There was a regional gradient between glacier outflow DOM composition and streamwater $\delta^{18}\text{O}$, suggesting covariation between regional precipitation gradients and the DOM exported from glacier outflows. Ultimately, this highlights that atmospheric deposition may exert a control on glacier outflow DOM composition, suggesting regional air circulation patterns and precipitation sources in part determine the origins and quality of OM exported from glacier environments.

Plain Language Summary The composition of Ecuadorian glacier dissolved organic matter (DOM) is unknown, despite its potential importance for downstream carbon cycling. Here, regional variability in the source, composition, and age of DOM in glacier surface and outflow streams was explored to identify drivers of variability in DOM composition across Ecuadorian glaciers. Ecuadorian glacier outflows exported aged material (2,730–910 yBP), that was available for microbial metabolism, and hence was associated with a DOM pool enriched in simple, energy-rich compounds. Nonetheless, regionally, dissolved organic carbon (DOC) in glacier outflows was older than in studied surface streams, perhaps indicating integration of compositionally diverse surface sources, or potentially aged organic matter (OM) from beneath the glaciers, in transit to the outflow. Across Ecuador, the age and molecular composition of DOM covaried, demonstrating changing contributions of compositionally diverse and variably aged OM sources to the glaciers. Regionally, a fraction of this variation was likely driven by atmospheric deposition to glacier surfaces. Given the rapid retreat of tropical glaciers and dearth of DOM compositional studies, future work must further constrain the origins of atmospheric deposition, since it may impact the quality of DOM exported to downstream ecosystems, potentially impacting its fate.

Supervision: Eran Hood, Robert G. M. Spencer

Visualization: Amy D. Holt, Robert G. M. Spencer

Writing – original draft: Amy D. Holt

Writing – review & editing: Amy D. Holt, Anne M. Kellerman, Tom. I. Battin, Amy M. McKenna, Eran Hood, Hannes Peter, Robert G. M. Spencer

1. Introduction

Mountain glaciers export dissolved organic carbon (DOC) to downstream ecosystems (global flux 0.58 ± 0.07 TgCyr⁻¹; Hood et al., 2015). Past studies, focused primarily on Tibet, Alaska, and the European Alps, have shown mountain glacier DOC to be ancient, highly bioavailable and assimilated into proglacial food webs (e.g., Fegél et al., 2019; Fellman, Hood, Raymond, Hudson, et al., 2015; Hood et al., 2009; Singer et al., 2012; Spencer, Guo, et al., 2014). Thus, glacier-derived dissolved organic matter (DOM) may play an important role in watershed biogeochemical cycling. Predicting impacts of glacier retreat on downstream biogeochemical dynamics requires constraints to be placed on how the composition of DOM in glacier outflows varies spatially and the sources of OM that underpin its composition.

Ultrahigh-resolution molecular level techniques have shown supraglacial and outflow DOM to be aliphatic-rich (i.e., high relative abundance of chemical formulae at H/C ≥ 1.5) and associated with elevated contributions of nitrogen and sulfur containing compounds compared to typical riverine DOM (e.g., Feng et al., 2016; Kellerman et al., 2021; Lawson et al., 2014; Singer et al., 2012; Spencer, Guo, et al., 2014; Stubbins et al., 2012). Proposed sources of OM to glacier ecosystems are diverse including atmospheric deposition of soil and combustion byproducts (e.g., from fossil fuels and biomass burning), subglacial OM (i.e., plant and soil OM overridden during glacier advance, and leached or mobilized by the passage of water through the subglacial hydrological system), and microbial OM from supraglacial or subglacial environments (Bhatia et al., 2010; Hood et al., 2009; Koch & Hansen, 2005; Magalhães et al., 2019; Singer et al., 2012; Spencer, Guo, et al., 2014; Stubbins et al., 2012). Photochemical degradation has been highlighted as a mechanism to explain how the deposition of ancient, highly aromatic (e.g., soil and fossil fuel combustion byproducts) OM to glacier surfaces may contribute to the ancient, aliphatic-rich properties observed for supraglacial and outflow DOM (Holt, Kellerman, et al., 2021). Additionally, biological processes on glacier surfaces may result in temporal and spatial variability in DOC concentrations and the presence of biolabile DOM compounds (Holland et al., 2019; Musilova et al., 2017; Nicholes et al., 2019). Similarly, the prevalence of different DOM pools appears to evolve in polythermal catchments with seasonal shifts in the hydrological system (Bhatia et al., 2010, 2013; Dubnick et al., 2017; Kellerman et al., 2020; Spencer, Vermilyea, et al., 2014), and the composition of glacier DOM has been shown to differ between glacier catchments, as well as across supraglacial environments and orographic precipitation gradients (Bhatia et al., 2010; Fellman, Hood, Raymond, Stubbins, & Spencer, 2015; Kellerman et al., 2021; Smith, Dieser, et al., 2018). Together these findings suggest a complex interplay of OM sources contributing to the DOM composition of glacier ecosystems, likely resulting in spatiotemporal nuances in the ancient, aliphatic, and highly bioavailable signature commonly observed in supraglacial ecosystems and glacier outflows.

To date, few studies have comprehensively assessed spatial variability in supraglacial and outflow DOM composition within and between regions (e.g., Kellerman et al., 2021; Singer et al., 2012; Svalbard and European Alps, respectively), and studies combining multiple analytical techniques (e.g., carbon isotopes, optical metrics, biomarkers and molecular level techniques) are also limited (e.g., Fellman, Hood, Raymond, Stubbins, & Spencer, 2015; Spencer, Guo, et al., 2014; Stubbins et al., 2012; Zhou et al., 2019). This hampers the capacity to understand regional variability in sources and composition of DOM being exported from glaciers. Past spatial assessments of DOM composition in glacier rivers in Asia and Alaska, have examined streamwater DOM composition across watersheds with gradients in glacier cover (e.g., Fellman et al., 2014; Hemingway et al., 2019; Hood et al., 2009; Zhou et al., 2019). Although these studies are useful for understanding changes to watershed DOM composition with shifting glacier coverage, glacier outflow DOM signatures can be overwhelmed by terrestrially-derived DOM from non-glacial, vegetated parts of the watershed (Behnke et al., 2020; Holt, Fellman, et al., 2021), making it difficult to tease apart differences in DOM chemistry and sources of OM between and within the glacier catchments themselves. Thus, studies utilizing multiple analytical techniques to assess DOM composition of supraglacial ecosystems and glacier outflows across a region are required to understand subtle changes in glacier DOM composition and source, to establish the potential drivers of the variation.

Tropical mountain glaciers are extremely vulnerable to climate change with rapid and accelerated glacier loss since the 1970s (Rabatel et al., 2013; Vuille et al., 2018; Zemp et al., 2019). Despite Ecuador housing a small fraction (4%) of the Andean tropical glaciers, they form part of the headwaters of the Amazon and provide a locally significant water resource (Rabatel et al., 2013). Importantly, large scale hydrological change, together with declining glacier-derived particulates, as well as organic and inorganic solutes, may impact the physico-chemistry of downstream proglacial lake, wetland and páramo (i.e., South American alpine tundra) ecosystems

(Barta et al., 2018; Buytaert et al., 2006, 2011). Despite the importance of glacier-derived solutes in high- and mid-latitude settings, the role glacier-derived DOM has on ecosystem and carbon dynamics in tropical watersheds has not been evaluated, and the composition and sources of DOM to Ecuadorian glacier ecosystems are unknown. Thus, assessing the variability in supraglacial and outflow DOM composition across the Ecuadorian Andes acts as a first step in elucidating its biogeochemical importance, in the face of rapid, unabated glacier retreat.

This study investigated the spatial variability in glacier DOM composition across ice capped volcanic mountains in the northern Andes, Ecuador. Samples were collected in 2020 during a 1-month sampling campaign (February–March). The DOM composition of supraglacial and outflow streams was assessed through bulk properties (DOC concentration and bioavailable DOC; BDOC), isotopic composition ($\delta^{13}\text{C}$ -DOC and $\Delta^{14}\text{C}$ -DOC), and molecular-level composition using negative-ion electrospray ionization ultrahigh-resolution 21 T Fourier transform ion cyclotron resonance mass spectrometry (FT-ICR MS). DOM compositional data were used in conjunction with streamwater isotopic ($\delta^{18}\text{O}$) analyses to examine whether outflow DOM composition was related to regional precipitation gradients, and could be linked to an atmospheric origin of glacier DOM. Ultimately, this provides insight into how atmospherically deposited OM impacts the composition of DOM exported from glacier ecosystems.

2. Materials and Methods

2.1. Study Area, Sampling, Processing, and Bioincubations

The climate of the Ecuadorian Andes is complex and influenced by air masses of Atlantic (arriving predominantly via the Amazon Basin) and Pacific origin. The precipitation distribution is characterized as bimodal (precipitation maxima March–May and October–November), driven by the north–south passage of the Intertropical Convergence Zone (Cauvy-Fraunié et al., 2013; Garcia et al., 1998). In comparison to precipitation, due to the proximity to the Equator, temperature remains relatively constant throughout the year, resulting in year-round ablation. Thus, these warm-based Ecuadorian glaciers have relatively constant mass balance and discharge compared to high-latitude, winter accumulation type glaciers (Benn & Evans, 2014; Cauvy-Fraunié et al., 2013; Gualco et al., 2022; Rabatel et al., 2013). For example, on Antisana, monthly average air temperatures at 4,850 m are between 0.5–2°C (period 2005–2010; Cauvy-Fraunié et al., 2013). El Niño–Southern Oscillation related changes in sea surface temperature in the tropical Pacific leads to interannual variability in precipitation and temperature, and thus glacier mass balance (Favier et al., 2004).

Samples were collected from February 5th to 1 March 2020 (i.e., beginning of wet season), from supraglacial ($n = 5$) and glacier outflow ($n = 14$) streams across five volcanoes (Table 1 and Figure 1). Supraglacial samples were collected from surface streams within the ablation zone and proximate to the glacier terminus. Outflow samples were collected ≤ 220 m (6–220 m) from the glacier terminus. There was limited time for in-stream processing between glacier terminus and outflow sampling sites due to short transit distances, cool waters, and high turbidity; hence, outflow streamwater samples are akin to those exiting the glacier. The majority of DOC and streamwater was from the glacier itself rather than other potential terrestrial sources (e.g., lateral inputs from moraine and vegetated slopes), since these sites are ice capped volcanoes, hence above our sampling points was glacier ice.

Streamwater samples were collected in acid-washed (10% HCl v/v 48hr) 1L HDPE Nalgene® bottles rinsed three times with streamwater before collection. Sample water was immediately filtered to 0.7 μm using pre-combusted (450°C, 5 h) GF/F filters in pre-rinsed, acid-washed polysulfone Nalgene® filter towers. An aliquot of 0.7 μm filtered streamwater from the glacier outflows ($n = 14$) was used for water isotope ($\delta^{18}\text{O}$) analysis. Samples for $\delta^{18}\text{O}$ were stored at room temperature (20°C) in 25 mL glass bottles with no headspace. Water isotopes were not collected for supraglacial streamwater samples. Samples for DOC concentration, $\delta^{13}\text{C}$ -DOC and $\Delta^{14}\text{C}$ -DOC were acidified to pH 2 (10 M HCl) and stored in pre-cleaned polycarbonate bottles in the dark on dry ice. These samples were returned to Florida State University and frozen (−20°C) until analysis.

For each supraglacial and outflow stream, 1 L of 0.7 μm filtered streamwater was collected into a pre-cleaned polycarbonate bottle, acidified to pH 2 (10 M HCl) and subsequently solid phase extracted in the field onto prepared 100 mg Bond-Elut PPL cartridges (Agilent Technologies Inc., Santa Clara, CA) for FT-ICR MS analysis (Dittmar et al., 2008). In brief, PPL cartridges were prepared in the laboratory by soaking overnight with one cartridge volume (3 mL) of HPLC grade methanol (MeOH), rinsing with 3 mL of MeOH and then rinsing

Table 1

Study Site Location and Elevation, Water Isotopic Signature, Dissolved Organic Carbon (DOC) Concentration, Bioavailable DOC (BDOC), and DOC Isotopes

Sample Type	Latitude (DD)	Longitude (DD)	Elevation (m)	$\delta^{18}\text{O}$ (‰)	DOC (mg C L ⁻¹)	BDOC (%)	$\delta^{13}\text{C}$ -DOC (‰)	$\Delta^{14}\text{C}$ -DOC (‰)	$\Delta^{14}\text{C}$ (yBP)
Outflow									
CH 1	-1.4462	-78.8040	4,936	-12.1	0.26	-	-27.1	-294.5	2,730
CAR 1	-1.4051	-78.7559	4,764	-12.5	0.26	42	-24.4	-247.1	2,210
CO 1	-0.6672	-78.4341	4,913	-11.6	0.31	-	-	-	-
CO 2	-0.6681	-78.4405	5,048	-12.3	0.27	-	-	-	-
CO 3	-0.6673	-78.4316	4,867	-12.0	0.26	-	-22.7	-179.5	1,520
CO 4	-0.6663	-78.4263	4,757	-12.7	0.22	-	-	-	-
AN 1	-0.4941	-78.1587	4,723	-13.9	1.08	81	-20.5	-114.5	910
AN 2	-0.4724	-78.1511	4,872	-12.6	0.24	-	-21.6	-116.4	925
AN 3	-0.4739	-78.1543	4,832	-12.5	0.34	-	-	-	-
AN 4	-0.4778	-78.1582	4,791	-13.2	0.34	-	-	-	-
CA 1	0.0161	-78.0055	4,894	-13.2	0.72	-	-21.0	-207.9	1,800
CA 2	0.0107	-78.0068	4,661	-13.0	0.58	72	-21.3	-195.1	1,680
CA 3	0.0167	-78.0065	4,861	-14.0	0.36	-	-20.5	-219.5	1,920
CA 4	0.0402	-77.9969	4,698	-13.4	0.20	-	-20.7	-182.2	1,550
Supraglacial									
CO 2 S1	-0.6686	-78.4404	5,058	-	0.57	-	-25.9	23.4	>Modern
AN 1 S1	-0.4937	-78.1576	4,751	-	0.48	-	-21.2	-71.9	530
AN 1 S2	-0.4934	-78.1580	4,744	-	0.24	-	-17.4	-31.0	185
CA 2 S1	0.0158	-78.0040	4,911	-	0.79	64	-22.1	-137.8	1,120
CA 2 S2	0.0156	-78.0048	4,893	-	0.61	54	-21.6	-89.4	685

Note. Isotopes and BDOC were measured on a subset of glacier samples (“-” indicates samples were not taken).

with 6 mL of pH 2 Milli-Q. The PPL were capped and chilled (5°C) after preparation to prevent the PPL resin from drying during the field campaign. Following extraction, the PPL were rinsed with 6 mL of pH 2 Milli-Q, to remove inorganics, and stored at 5°C.

To determine BDOC, a subset of supraglacial ($n = 2$) and outflow ($n = 3$) 0.7 μm filtered streamwaters were incubated, in precleaned 120 mL polycarbonate bottles, at 20°C in the dark (Spencer, Guo, et al., 2014). Incubations were conducted in triplicate. Each incubation lasted 28-day, at which point samples were filtered using a syringe and filter capsule equipped with a pre-combusted 0.7 μm GF/F filter. Samples were acidified to pH 2 (10M HCl) and frozen, at -20°C, until DOC analysis (Fellman et al., 2010; Spencer, Guo, et al., 2014). BDOC (%) was calculated as the percentage difference in DOC before and after the 28-day incubation (Fellman et al., 2008).

2.2. Water Isotopes

Outflow samples were analyzed for water isotopes ($\delta^{18}\text{O}$) on a Picarro 2140-i Wavelength-Scanned Cavity Ring Down Spectrometer (Picarro Inc., Santa Clara, California, USA) in the Stable Isotope Laboratory of the University of Lausanne, Switzerland. Results were normalized to Vienna Standard Mean Ocean Water. Variability in $\delta^{18}\text{O}$ can be used to assess spatial gradients in precipitation as well as its source(s), and thus variation in the possible source(s) of atmospheric deposition (including of DOM compounds) to glacier surfaces (Cabrera et al., 2022; Fellman, Hood, Raymond, Stubbins, & Spencer, 2015; Garcia et al., 1998; Ginot et al., 2002).

2.3. DOC Concentration and Isotopic Analyses

Concentrations of DOC were measured on a Shimadzu TOC-L CPH analyzer, using a five-point potassium hydrogen phthalate calibration curve that covered the samples concentration range (R^2 0.999). Three to seven

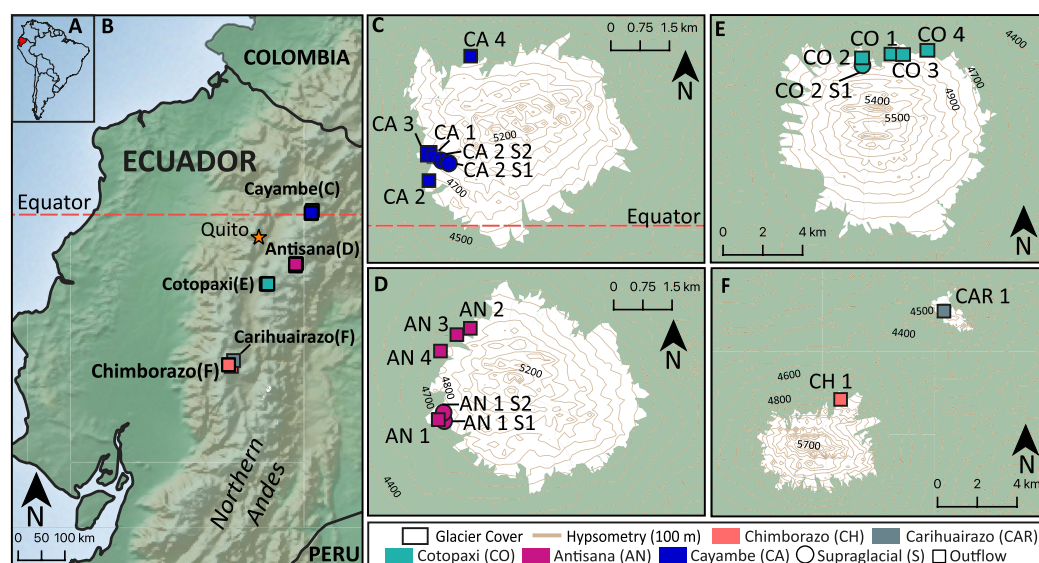


Figure 1. Location of 2020 sample sites (a) location of Ecuador within South America, (b) study volcanoes, (c–f) individual volcanoes, with samples sites abbreviated (see key for details). Map data: glacier cover (delineation year 2000) from Global Land Ice Measurements (GLIMS; <http://www.glims.org/>), land boundaries and topography Natural Earth (<https://www.naturalearthdata.com/>), and hypsometric contours created using Google Earth Pro, GPS visualizer (<https://www.gpsvisualizer.com/>) and QGIS (inverse distance weighted interpolation processing tool).

replicate injections (150 μL) were averaged and had a coefficient of variance $<2\%$. Aliquots of deep-sea reference material (Batch 17 Lot 04–17; Carbon Reference Materials, University of Miami, Rosenstiel School of Marine and Atmospheric Sciences) were analyzed to ensure precision and accuracy. Measured values were within 5% of reported concentrations. A subset of supraglacial and outflow samples ($n = 5$ and 9, respectively) were analyzed for stable and radiogenic carbon isotopes ($\delta^{13}\text{C}$ -DOC and $\Delta^{14}\text{C}$ -DOC, respectively) at the National Ocean Sciences Accelerator Mass Spectrometry (AMS) Facility at Woods Hole Oceanographic Institution, USA (Roberts et al., 2010; Xu et al., 2021, 2022). Briefly, DOC was UV-oxidized, and resultant CO_2 cryogenically purified and analyzed for $\Delta^{14}\text{C}$ -DOC. The $\Delta^{14}\text{C}$ -DOC values were corrected for $\delta^{13}\text{C}$ using AMS measurements. A split of CO_2 was measured for $\delta^{13}\text{C}$ -DOC on a stable isotope ratio mass spectrometer (Gospodinova et al., 2016; Griffith et al., 2012; Xu et al., 2021).

2.4. Fourier Ion Cyclotron Resonance Mass Spectrometry

Field extracted PPL cartridges were dried with a flow of ultrahigh purity nitrogen gas and eluted with HPLC grade MeOH into pre-combusted (550°C, 5 h) glass vials (2 or 4 mL). The volume of MeOH used in each elution was adjusted dependent on the DOC concentration of the sample, to achieve a target eluent concentration of 50 $\mu\text{g C mL}^{-1}$ assuming an extraction efficiency of 40% (Dittmar et al., 2008). Samples were stored at -20°C until analysis.

Molecular level DOM composition was analyzed using negative-ion electrospray ionization on a 21 T FT-ICR MS at the National High Magnetic Field Laboratory, Florida, USA (Hendrickson et al., 2015; Smith, Podgorski, et al., 2018). For each samples mass spectrum 100 scans were conditionally co-added, phase-corrected, and internally calibrated with 10–15 highly abundant homologous series that spanned the entire molecular weight distribution based on the “walking” calibration in Predator analysis, only peaks with a signal greater than the root mean square baseline noise plus 6σ were exported to a peak list (Blakney et al., 2011; Savory et al., 2011). Elemental compositions were assigned between ≥ 170 and $\leq 1,200$ Da, within the elemental bounds $\text{C}_{1-100}\text{H}_{4-200}\text{O}_{1-30}\text{N}_{0-4}\text{S}_{0-2}$ (error ± 0.3 ppm) using PetroOrg© (Corilo, 2014). The relative abundance (RA) of individual peaks was calculated as the percent contribution of a peak as a fraction of the total intensity of all assigned peaks in a sample, scaled to 10,000.

Molecular formulae were classed according to heteroatomic content. Formulae containing only carbon, hydrogen and oxygen were classed as CHO, and these elements with the addition of nitrogen and/or sulfur were classed as CHON, CHOS and CHONS. The nominal oxidation state of carbon (NOSC) and modified aromaticity index (AI_{mod}) was calculated for each neutral elemental composition (Koch and Dittmar 2006, 2016; Riedel et al., 2012). The NOSC can be used to understand biogeochemical reactivity and biolability of a compound, and AI_{mod} is a metric of aromaticity (LaRowe & Van Cappellen, 2011; Riedel et al., 2012). Based on AI_{mod} and elemental ratios (H/C and O/C) structural features of individual formulae can be inferred (Koch & Dittmar, 2006). Nonetheless, specific structural configuration is not afforded through elemental composition derived from FT-ICR MS analysis and hence each formula may represent numerous structural isomers (Hertkorn et al., 2007; Kellerman et al., 2021; Koch & Dittmar, 2006). Thus, formulae were categorized into six operationally-defined compound classes based on stoichiometry and AI_{mod} : polyphenolic and condensed aromatics (AI_{mod} values of 0.5–0.67 and >0.67, respectively), highly unsaturated and phenolic (HUP; AI_{mod} of <0.5 and H/C < 1.5), aliphatic (H/C \geq 1.5, O/C \leq 0.9 and $N = 0$), peptide-like (H/C \geq 1.5, O/C \leq 0.9 and $N > 0$), and sugar-like (H/C \geq 1.5–2 and O/C > 0.9; Kellerman et al., 2021; Spencer, Guo, et al., 2014). The RA of each class was calculated as the total RA of all peaks belonging to that class. Sugar-like compounds made up <1% of all samples RA and thus are not discussed further.

2.5. Statistical Analyses

All statistical analyses were carried out using R Version 1.1.463 (R Core Team, 2020). An analysis of variance test was used to assess the difference in DOC, $\delta^{13}C$ -DOC, $\Delta^{14}C$ -DOC and FT-ICR MS metrics between supraglacial and outflow streams. Linear regression analysis was performed between FT-ICR MS metrics and $\Delta^{14}C$ -DOC and $\delta^{18}O$, respectively. An analysis of covariance (ANCOVA) test was used to assess the effect of sample type (i.e., supraglacial or outflow stream) on $\Delta^{14}C$ -DOC regressions. Principal component (PC) analyses were conducted using the FactoMineR package (Lê et al., 2008), to assess spatial gradients in outflow DOM composition, source, and age across the region. Two PC analyses were performed to incorporate carbon isotope data into the spatial assessment. The first PC analysis included all outflows and considered $\delta^{18}O$, DOC, and RA weighted FT-ICR MS parameters. The second PC analysis included $\delta^{13}C$ -DOC and $\Delta^{14}C$ -DOC in addition to those variables in the first analysis and thus included only outflow streams with carbon isotope data ($n = 9$). It was not possible to conduct only one PC analysis, since the mean carbon isotopic value of the data set would have been applied to those samples where $\delta^{13}C$ -DOC and $\Delta^{14}C$ -DOC was not measured, distorting the analysis. Mean RA weighted mass was removed from both PC analyses as, in each case, it was an insignificant driver of PC1 and 2.

3. Results

3.1. Water Isotopic Signatures of Outflow Streams

Glacier outflow $\delta^{18}O$ values ranged from -14.0 to -11.6‰ (Table 1 and Figure 2). Outflow streamwater was likely a mixture of runoff from precipitation, snowmelt, and glacier (supraglacial and basal) ice melt, and thus streamwater isotopic signatures likely represented an integrated signature of multiple years of precipitation. Given this, the isotopic signal of each meltwater component and the fraction of streamflow it contributed to an outflow could vary across the sample sites. As such, despite their proximity, there was slight variability in isotopic signatures of outflow samples for individual volcanoes ($\leq 1.4\text{‰}$; Table 1 and Figure 2). The most $\delta^{18}O$ depleted values were observed in the northern volcanoes of Cayambe and Antisana and enriched values found in southern catchments (Figure 2). There was no trend in $\delta^{18}O$ with elevation between the sample sites, instead from south to north $\delta^{18}O$ values typically became more depleted (Figure 2).

3.2. Bulk DOC Properties of Supraglacial and Outflow Streams

The concentrations of DOC were comparable between supraglacial (0.24 – 0.79 mg C L⁻¹) and outflow (0.20 – 1.08 mg C L⁻¹) streams, and 42%–81% ($n = 5$) of DOC was biolabile (Table 1 and Figure 3a). There was considerable variability in $\delta^{13}C$ -DOC signatures across the region, particularly within supraglacial streams (range -25.9 to -17.4 and -27.1 to -20.5‰ for supraglacial and outflow streams, respectively; Figure 3b). However, there was no difference in $\delta^{13}C$ -DOC between supraglacial and outflow streams (Figure 3b). The radiocarbon ages ($\Delta^{14}C$ -DOC) across the region ranged from 2,730 yBP to > modern (-294.5 to 23.4‰ , respectively). Supraglacial streams were significantly more enriched in $\Delta^{14}C$ -DOC (i.e., younger) than the outflows (mean -61.3

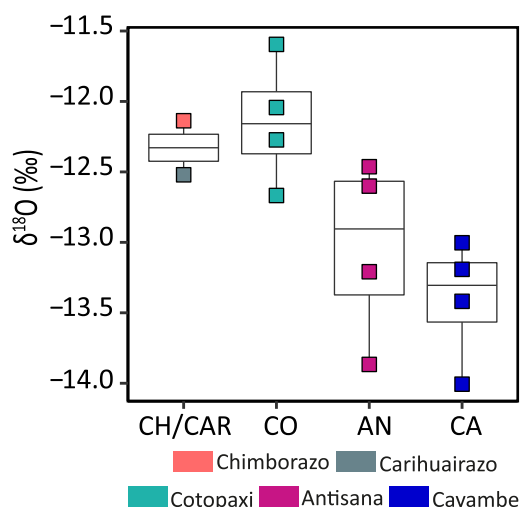


Figure 2. Water isotopic ($\delta^{18}\text{O}$) signature of each glacier outflow. Individual data points plotted and colored by volcano. Note that water isotopes were not measured for supraglacial samples.

and -195.2‰ respectively; Table 1 and Figure 3c). This systematic offset in $\Delta^{14}\text{C-DOC}$ between supraglacial and outflow streams occurred in spite of overlapping DOC concentrations and $\delta^{13}\text{C-DOC}$ signatures (Figure 3).

3.3. Molecular Level DOM Composition

Across the data set there were 20,318 unique formulae, and between 2,394 and 11,950 formulae were assigned for individual samples (Table 2). There was no systematic difference in the number of assignments between supraglacial and outflow samples, and a substantial number of formulae were shared between supraglacial streams and their respective outflows (3,641 to 7,840 formulae). Typically, supraglacial DOM had a larger and less variable mean RA weighted mass than the outflows (503.88 ± 8.45 and 469.77 ± 21.17 Da, respectively; Table 2). The RA of heteroatom classes was variable across the data set: CHO ($33.7\text{--}73.8\%$ RA), CHON ($7.7\text{--}24.3\%$ RA), CHOS ($4.6\text{--}50.3\%$ RA) and CHONS ($0\text{--}4.0\%$ RA; Table 1 and Figures 4a–4c). There was no significant difference in any of the heteroatom classes between supraglacial and outflow streams, although O/C ratios were slightly higher for supraglacial DOM (mean 0.47 ± 0.01 and 0.44 ± 0.02 , supraglacial and outflow respectively; Table 1 and Figures 4a–4c).

Aromaticity was low, yet variable across the region (AI_{mod} 0.10–0.22), where condensed aromatic and polyphenolic compounds made up a minor fraction of DOM composition (combined 1.3–7.6%RA; Table 2 and Figure 4d). On average, supraglacial DOM contained marginally more condensed aromatic and polyphenolic compounds than outflow DOM (combined mean 4.0 ± 2.4 and $2.0 \pm 2.4\%$ RA, respectively), but bulk aromaticity was comparable (mean AI_{mod} 0.15 ± 0.05 and 0.15 ± 0.03 , respectively; Table 2 and Figure 4d). HUP compounds were a dominant fraction of supraglacial and outflow streamwater DOM composition and ranged from 37.2 to 69.7%RA across the region (Table 2 and Figure 4e). No difference in HUP content was found between supraglacial and outflow streams (Figure 4e). Mean RA weighted H/C ratios and NOSC ranged from 1.30 to 1.51 and -0.62 to -0.31 respectively, highlighting the prevalence of aliphatic and peptide-like compounds across the data set (Table 2). On average, supraglacial streams had a higher NOSC than outflow streams (mean -0.40 ± 0.08 and -0.49 ± 0.06 , respectively; Table 2). Nevertheless, there was no significant difference in H/C ratio or aliphatic and peptide-like content between supraglacial and outflow DOM (combined mean 45.5 ± 12.0 and $44.0 \pm 7.5\%$ RA, respectively; Table 2 and Figure 4f). As for isotopic values, heteroatom content, AI_{mod} and the %RA of HUP compounds, there was a large range in the %RA of aliphatic and peptide-like formulae across the region (combined 27.1–61.1%RA; Tables 1 and 2; Figures 3 and 4). Overall, although at the molecular level there was considerable compositional similarity between supraglacial and outflow streamwater samples, there was a substantial range in DOM composition across Ecuadorian volcanoes, suggesting regional variability in molecular level glacier DOM composition.

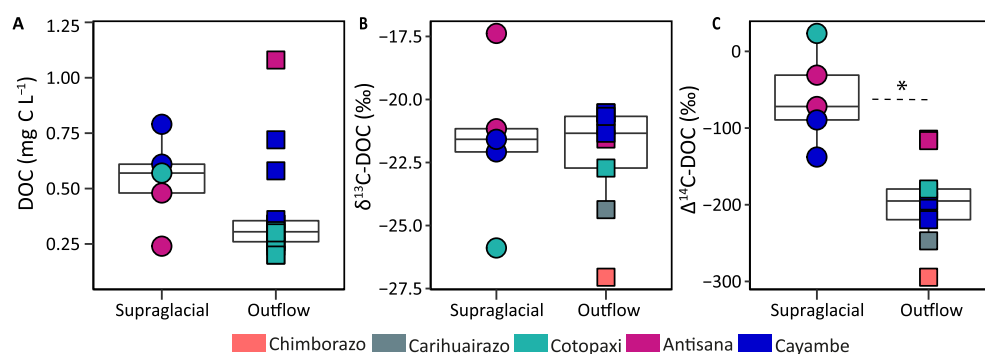


Figure 3. (a) Dissolved organic carbon (DOC) concentration, and (b and c) carbon isotopic signatures ($\delta^{13}\text{C-DOC}$ and $\Delta^{14}\text{C-DOC}$) separated by sample type. Individual data points are shaped and colored according to sample type and volcano, respectively (see key for details). Asterisk denotes significant difference in $\Delta^{14}\text{C-DOC}$ values between supraglacial and outflow samples.

Table 2
Number of Formulae and Relative Abundance (RA) Weighted Mass, H/C and O/C Ratio, Nominal Oxidation State of Carbon (NOSC), and Modified Aromaticity Index (AI_{mod}), Together With the Percent RA of Each Compound and Heteroatom Class

Sample type	Formulae (#)	Mass (Da)	H/C	O/C	NOSC	AI_{mod}	Condensed			Aliphatic (%RA)	Peptide-like (%RA)	CHO (%RA)	CHON (%RA)	CHOS (%RA)	CHONS (%RA)
							HUPs (%RA)	aromatic (%RA)	Polyphenolic (%RA)						
Outflow															
CH 1	2,394	418.28	1.35	0.42	-0.47	0.21	69.7	0.2	3.0	20.6	6.5	73.8	21.6	4.6	0.0
CAR 1	9,974	471.03	1.37	0.44	-0.43	0.18	62.0	0.3	2.7	29.3	5.6	65.3	21.6	12.4	0.7
CO 1	11,950	489.81	1.39	0.45	-0.41	0.16	61.9	0.2	1.8	30.1	5.9	63.9	24.0	11.3	0.8
CO 2	10,248	480.62	1.45	0.45	-0.45	0.13	50.7	0.1	1.2	39.4	8.4	45.3	24.3	28.9	1.5
CO 3	8,075	458.78	1.45	0.41	-0.56	0.14	50.2	0.1	1.6	40.1	7.8	58.8	15.6	22.8	2.8
CO 4	10,067	485.14	1.45	0.46	-0.47	0.13	51.3	0.2	1.3	34.7	12.2	60.6	24.2	13.8	1.5
AN 1	3,974	452.60	1.50	0.42	-0.62	0.12	39.7	0.1	1.7	49.5	8.9	67.9	9.5	21.4	1.1
AN 2	7,344	469.31	1.45	0.45	-0.51	0.14	53.3	0.2	1.1	34.1	10.8	69.9	21.5	8.6	0.0
AN 3	5,242	447.25	1.41	0.44	-0.47	0.17	56.0	0.2	2.2	29.7	11.7	67.0	23.8	9.2	0.0
AN 4	5,973	466.94	1.44	0.45	-0.48	0.13	52.2	0.2	1.7	39.3	6.4	42.5	7.7	46.6	3.3
CA 1	7,196	501.25	1.48	0.43	-0.55	0.11	48.0	0.1	1.5	44.5	5.4	39.7	8.0	50.3	2.1
CA 2	6,998	477.44	1.44	0.43	-0.51	0.14	52.5	0.1	2.0	38.7	6.3	42.6	10.5	44.8	2.1
CA 3	9,602	490.54	1.43	0.47	-0.43	0.14	53.4	0.3	1.8	35.3	8.2	55.8	17.2	26.2	0.8
CA 4	6,136	467.78	1.44	0.45	-0.47	0.13	52.1	0.2	1.7	39.3	6.4	42.3	7.9	46.6	3.2
Supraglacial															
CO 2 S1	9,930	500.61	1.51	0.47	-0.49	0.10	37.2	0.2	1.4	53.9	7.2	33.7	13.7	48.6	4.0
AN 1 S1	7,428	502.15	1.44	0.47	-0.44	0.13	49.8	0.4	1.9	39.1	8.4	58.0	11.2	28.1	2.7
AN 1 S2	7,172	518.76	1.44	0.47	-0.44	0.13	45.9	0.7	2.6	41.9	8.6	60.8	9.8	26.4	3.1
CA 2 S1	11,267	499.85	1.30	0.47	-0.31	0.22	63.0	1.8	5.8	23.0	6.3	68.7	17.5	13.0	0.7
CA 2 S2	9,180	498.04	1.36	0.50	-0.32	0.17	55.5	1.1	4.1	30.8	8.3	66.4	15.2	16.6	1.9

3.4. Trends in Molecular Level DOM Composition

Molecular level DOM properties were highly correlated with $\Delta^{14}\text{C}$ -DOC for both supraglacial and outflow streams, with a clear and significant age offset shifted to $\Delta^{14}\text{C}$ enrichment in supraglacial samples (Figure 5). The gradient of change in molecular level composition was statistically indistinguishable between sample types (Figure 5). As supraglacial and outflow DOC became $\Delta^{14}\text{C}$ enriched, DOM had decreased aromaticity (i.e., lower AI_{mod}), with a decreased %RA of HUP compounds and an increased %RA of aliphatic and peptide-like formulae (Figure 5). The decrease in AI_{mod} associated with $\Delta^{14}\text{C}$ -DOC enrichment in supraglacial and outflow streams was largely a reflection of decreasing %RA of HUP and polyphenolic compounds, since condensed aromatic formulae were a minor fraction of total RA ($\leq 1.8\%$ and $\leq 0.3\%$ in supraglacial and outflows streams, respectively) that did not correlate with $\Delta^{14}\text{C}$ -DOC (Tables 1 and 2). For outflow streams, enrichment in $\Delta^{14}\text{C}$ -DOC was met with $\delta^{13}\text{C}$ -DOC enrichment (R^2 0.46, p -value 0.03). No such trend existed for supraglacial samples. Except for sample CO2S1, individual supraglacial samples, although younger, had higher aromaticity and %RA of HUP compounds, with lower aliphatic and peptide-like content than their respective outflow (Table 2). This was surprising given the trend toward increased aliphatic and peptide-like content with $\Delta^{14}\text{C}$ -DOC enrichment in both supraglacial and outflow streams (Figure 5). Nonetheless, when supraglacial and outflow samples were compared across the data set, molecular level DOM composition was similar between the sample types, with a significant age offset (Figures 4 and 5).

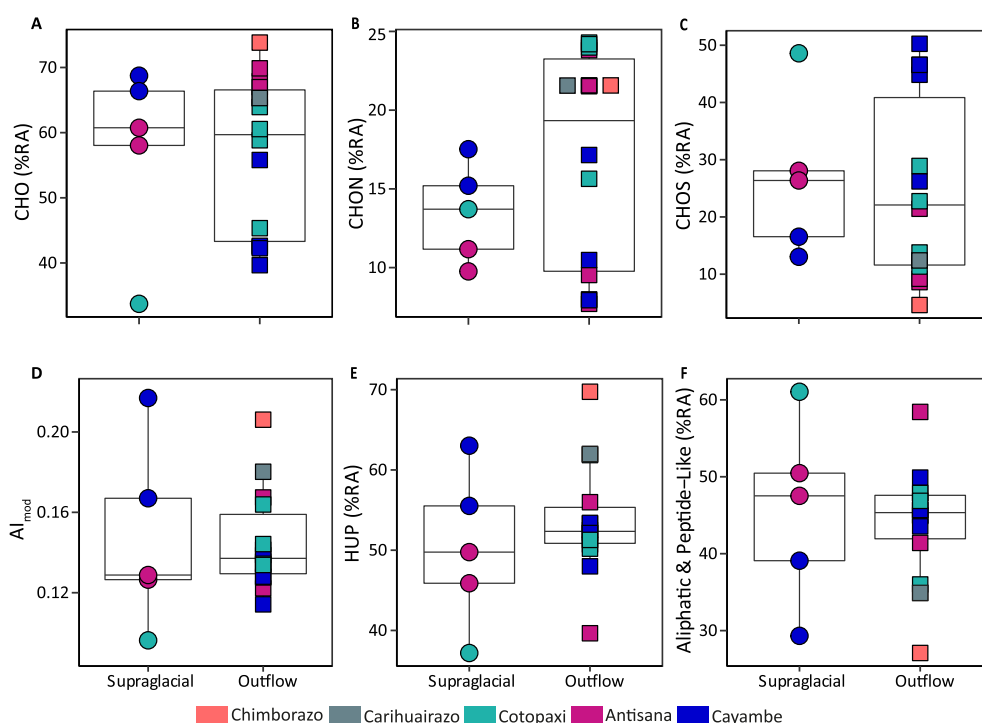


Figure 4. Molecular level dissolved organic matter (DOM) composition as determined by Fourier ion cyclotron resonance mass spectrometry (FT-ICR MS), separated by sample type. (a–c) The percent relative abundance (% RA) of each heteroatom class, (d) RA weighted modified aromaticity index (AI_{mod}), compound class scores for highly unsaturated and phenolic (HUP), and aliphatic and peptide-like compounds (E and F, respectively). Individual data points are shaped and colored according to sample type and volcano, respectively (see key for details).

Two principal component (PC) analyses were conducted to assess regional trends in molecular and isotopic composition of DOM in glacier outflows across the Ecuadorian Andes (Figure 6). PC analysis 1 considered DOC concentration, FT-ICR MS metrics, and $\delta^{18}O$. The second PC analysis included carbon isotope data as well as the variables in the first PC analysis, and thus was constrained to the nine outflow samples taken for carbon isotopes (Figure 6c). PC analysis 1 and 2 indicated regional trends in glacier outflow DOM composition with streamwater $\delta^{18}O$ (Table S1 in Supporting Information S1 and Figure 6). PC1 explained 52.6% and 60.0% of the variability in the data set for PC analysis 1 and 2 respectively. FT-ICR MS metrics clustered in PC space along lines of aromaticity in both analyses (Figure 6). Accordingly, in each case, PC1 was negatively correlated with the %RA of aliphatic and peptide-like compounds together with H/C ratios, whilst being strongly positively correlated with the %RA of HUP compounds and AI_{mod} . Across the region, molecular level DOM properties of glacier outflows were correlated with streamwater $\delta^{18}O$ (R^2 0.25–0.3, p -value 0.03–0.04; Figure 7). As streamwater $\delta^{18}O$ became enriched, DOM had higher aromaticity and %RA of HUP compounds, concomitantly the %RA of aliphatic compounds declined (Tables 1 and 2; Figures 7a and 7b). As such, PC1 was positively associated with $\delta^{18}O$ (Figure 6), and where data were available, negatively associated with $\Delta^{14}C$ -DOC (Figure 6c). Samples were distributed across PC1, reflecting the range in DOM and water isotopic composition across the Ecuadorian Andes (Figure 6). Typically, $\delta^{18}O$ values became more depleted toward the north of the study region (Figure 2). PC analysis and correlations of streamwater $\delta^{18}O$ with molecular level metrics showed that DOM concomitantly decreased in aromaticity and became enriched in aliphatic and peptide-like compounds (Figures 6 and 7). Aliphatic enriched DOM and streamwater $\delta^{18}O$ depletion was generally associated with enriched $\Delta^{14}C$ -DOC (i.e., younger; Figure 6). These correlations between DOM compositional metrics and streamwater $\delta^{18}O$ suggested that precipitation gradients across the Ecuadorian Andes may in part contribute to the variability in isotopic and molecular level composition of glacier outflow DOM.

In both PC analyses (i.e., PC analysis 1 and 2 with and without the addition of carbon isotopic data, respectively), PC2 explained considerably less variability in the data set than PC1 (17.7% and 18.4% for PC analysis 1 and

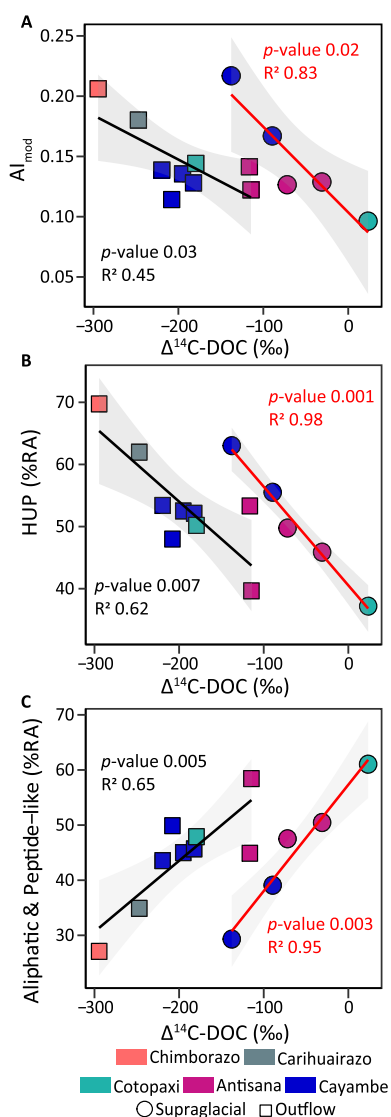


Figure 5. Association between molecular level dissolved organic matter (DOM) composition and $\Delta^{14}\text{C-DOC}$. (a) Relative abundance (RA) weighted modified aromaticity index (AI_{mod}), (b and c) the percent RA of highly unsaturated and phenolic (HUP), and aliphatic and peptide-like compounds, respectively. Points are shaped and colored according to sample type and volcano, respectively. Solid black and red lines indicate the respective linear regressions for outflow and supraglacial samples. Shading represents 95% confidence of regression.

2, respectively; Figure 6). Unlike PC1, PC2 was not as strongly associated with $\delta^{18}\text{O}$ (Table S1 in Supporting Information S1), and largely represented variability in NOSC, O/C ratios, and in the case of PC analysis 2 the %RA of condensed aromatic compounds (Table S1 in Supporting Information S1). PC2 likely reflected intrinsic variability in DOM quality and quantity (e.g., variability in the degree of bio- and photodegradation, spatiotemporal variability in the relative importance of atmospheric deposition events, and microbial activity).

4. Discussion

Bulk, isotopic, and molecular level analysis showed that overall Ecuadorian supraglacial and outflow streams exhibited similar properties to that observed for glacier-derived DOM in other regions (e.g., Bhatia et al., 2013; Hood et al., 2009; Singer et al., 2012; Spencer, Guo, et al., 2014). The glacier outflow streams in this study had low concentrations of DOC ($0.39 \pm 0.25 \text{ mg C L}^{-1}$ compared to a global mean of mountain glacier meltwaters of $0.4 \pm 0.1 \text{ mg C L}^{-1}$, $n = 55$; Table 1 and Figure 3a; Hood et al., 2009; Hood et al., 2015; Textor et al., 2018) that was highly biolabile (42%–81%; Table 1). Moreover, Ecuadorian glacier-derived DOM had low aromaticity and elevated heteroatom, aliphatic and peptide-like content compared to non-glacial rivers (Table 2 and Figure 4; Kellerman et al., 2021). Typically, <10% of RA is assigned to aliphatic formulae in non-glacial rivers (Behnke et al., 2021; Kellerman et al., 2021; Kurek et al., 2022), whereas Ecuadorian supraglacial and outflow streamwater DOM contained substantially more aliphatic compounds ($36.5 \pm 8.3\% \text{ RA}$, Table 2 and Figure 4f), in broad agreement with that observed for other glacier ecosystems examined globally ($27.3 \pm 24.3\% \text{ RA}$, $n = 96$; Behnke et al., 2020; Bhatia et al., 2010; Feng et al., 2016; Hemingway et al., 2019; Kellerman et al., 2021; Lawson et al., 2014; Spencer, Guo, et al., 2014; Stubbins et al., 2012).

Glacier $\delta^{13}\text{C-DOC}$ values reported in the literature were highly variable and ranged from -29.8 to -22‰ (mean $-25.3 \pm 1.8\text{‰}$, $n = 80$; Andrews et al., 2018; Behnke et al., 2020; Bhatia et al., 2013; Csank et al., 2019; Fellman, Hood, Raymond, Stubbins, & Spencer, 2015; Fellman et al., 2014; Fellman et al., 2010; Holding et al., 2017; Hood et al., 2009; Spencer, Guo, et al., 2014), whereas Ecuadorian glacier DOC was typically more enriched with a mean of $-22.0 \pm 2.4\text{‰}$ (range -27.1 to -17.4‰). Ecuadorian glacier DOC was on average ancient ($\Delta^{14}\text{C-DOC} -147.4 \pm 87.2\text{‰}$, Table 1 and Figure 3c). However, it was at the younger (i.e., more enriched) end of the age spectrum that has been observed across mid- to high-latitude glacier ecosystems (range -743 to -45‰ , mean $-361.1 \pm 164.7\text{‰}$, $n = 94$; Aiken et al., 2014; Andrews et al., 2018; Arimitsu et al., 2018; Behnke et al., 2020; Bhatia et al., 2013; Csank et al., 2019; Fellman, Hood, Raymond, Stubbins, & Spencer, 2015; Hood et al., 2009; Singer et al., 2012; Spencer, Guo,

et al., 2014), and one supraglacial stream had a modern isotopic signature ($\text{CO}_2\text{S1 } 23.4\text{‰}$; Table 1 and Figure 3c). Based on a simple mixing model, and assuming DOC is only derived from modern or $\Delta^{14}\text{C}$ dead ($\geq 50,000$ yBP, $-1,000\text{‰}$) sources, across the region bulk glacier DOC could contain 0%–28.8% fossil carbon. Although this is a simplification because DOC could be made up of a cocktail of OM sources of varying radiocarbon age, these values highlight the prevalence of near-modern to modern carbon in the make-up of this Ecuadorian supraglacial and outflow DOC. This contrasts with glacierized regions like southeast Alaska, where $\sim 75\%$ of glacier-derived DOC could feasibly be from a $\Delta^{14}\text{C}$ dead source, such as fossil fuel combustion byproducts (Fellman, Hood, Raymond, Stubbins, & Spencer, 2015; Stubbins et al., 2012).

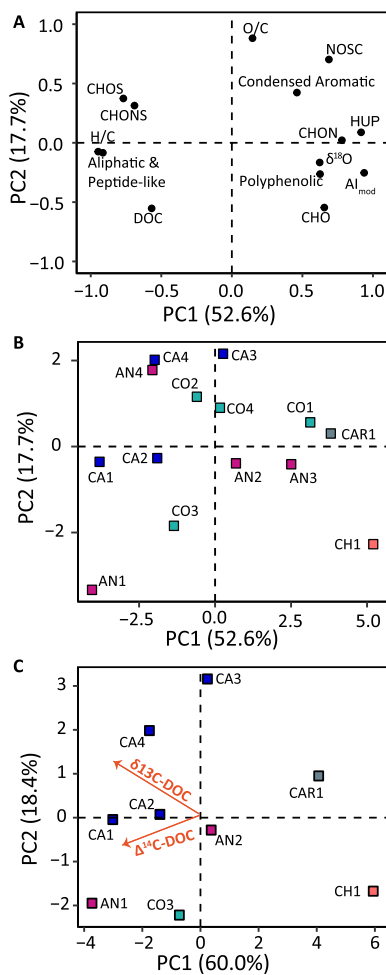


Figure 6. (a, b) principal component (PC) analysis for all outflow streams ($n = 14$) based on water isotopes, dissolved organic carbon (DOC) concentration and Fourier ion cyclotron resonance mass spectrometry (FT-ICR MS) parameters. (a) Loading plot of different variables and (b) scores plot of samples. (c) PC analysis scores plot, where $\delta^{13}\text{C-DOC}$ and $\Delta^{14}\text{C-DOC}$ were added as additional variables to those variables in (a). Note the analysis is confined to only those outflows with $\delta^{13}\text{C-DOC}$ and $\Delta^{14}\text{C-DOC}$ measurements ($n = 9$). The direction of correlation with $\delta^{13}\text{C-DOC}$ and $\Delta^{14}\text{C-DOC}$ is indicated by orange arrows. There was similarity in relative position of outflow streams along PC1 in (b) and (c). Structure matrix for each PC analysis (Table S1 in Supporting Information S1).

4.1. Variable Composition, Sources, and Age of Ecuadorian Glacier DOM

Ecuadorian supraglacial and outflow streamwater DOM was a mixture of aged to modern OM sources, that vary in relative proportions across the region, as shown by the large range in $\Delta^{14}\text{C-DOC}$ and correlation of $\Delta^{14}\text{C-DOC}$ with molecular level DOM composition (Tables 1 and 2; Figures 3–5). The shift in molecular level composition toward increased %RA of aliphatic and peptide-like compounds with $\Delta^{14}\text{C-DOC}$ enrichment could have been produced by an increased relative contribution of modern, recently fixed OM to the DOM pool (Figure 5). Similar positive correlations between $\Delta^{14}\text{C-DOC}$ and aliphatic formulae have been noted previously in the European Alps, where modern OM from microbes is suggested as a source of aliphatic compounds (Singer et al., 2012). Although $\delta^{13}\text{C}$ values are not known to have been published for microbial end-members in glacier ecosystems, the $\delta^{13}\text{C}$ of sea ice algae ranges from -21 to -16‰ , overlapping with that of Ecuadorian glacier DOC (Table 1 and Figure 3b; Hobson & Welch, 1992; McMahon et al., 2006). Given the positive correlation between $\delta^{13}\text{C}$ and $\Delta^{14}\text{C-DOC}$ in Ecuadorian outflows (R^2 0.46, p -value 0.03) and that microbes are found across glacier ecosystems producing low aromaticity DOM compounds (Hodson et al., 2008; Musilova et al., 2017), $\Delta^{14}\text{C-DOC}$ enriched glacier outflows could reflect a trend toward ice algal dominated $\delta^{13}\text{C-DOC}$ and molecular level DOM composition (Table 1 and Figure 5).

Nonetheless, the $\delta^{13}\text{C-DOC}$ signatures in supraglacial streams were variable across small age gradients, indicating multiple sources of recently fixed carbon may have contributed to supraglacial and outflow DOM composition (Table 1 and Figure 3). For example, the two most enriched $\Delta^{14}\text{C-DOC}$ streamwater samples (CO2S1 and AN1S2, $\Delta^{14}\text{C-DOC}$ 23.4 and -31‰ , respectively) covered 88% of the observed $\delta^{13}\text{C-DOC}$ range (-27.1 to -17.4‰), despite representing only 17% of the $\Delta^{14}\text{C-DOC}$ range (-294.5 to 23.4‰ ; Table 1). The neighboring páramo and Amazon Basin are dominated by C3 vegetation ($\delta^{13}\text{C}$ of C3 plants globally ranges from -37 to -20‰ , mean -28.5‰ Boom et al., 2001; Kohn, 2010; Powell & Still, 2009). Thus, atmospheric deposition of OM derived from pollen, plant material, and burnt biomass may have contributed modern, $\delta^{13}\text{C}$ depleted carbon to glacier surfaces, explaining relatively enriched $\Delta^{14}\text{C-DOC}$, but depleted $\delta^{13}\text{C-DOC}$ signatures (e.g., CO2S1; Table 1). Pollen and biomass burning tracers have been detected on the surface and in ice cores of Ecuadorian glaciers, respectively (Ginot et al., 2002; Ledru et al., 2013). Furthermore, pollen-derived DOM has been shown to produce fluorophores at short excitation and emission wavelengths (Mladenov et al., 2011), and hence is likely to be proteinaceous in character, similar to that observed for glacier-DOM (Table 1; Fellman, Hood, Raymond, Stubbins, & Spencer, 2015; Hood et al., 2009; Kellerman et al., 2020).

Similarly, though relatively distant, wildfires or pollen from C4 dominated grasslands of the ecotones of the Amazon rainforest and savanna may have contributed modern OM with enriched $\delta^{13}\text{C-DOC}$ signatures to Ecuadorian glacier surfaces ($\delta^{13}\text{C}$ of C4 plants globally range from -14 to -10‰ ; Cerling et al., 1997). It is unclear whether C3 or C4 vegetation dominates continental biomass emissions, despite fires occurring predominantly in regions associated with recent deforestation or high percentage cover of C4 grasses (Chen et al., 2013; Powell & Still, 2009). Nonetheless, atmospheric deposition of plant OM or biomass burning byproducts could explain the trends between $\Delta^{14}\text{C-DOC}$ and molecular level DOM composition seen across the Ecuadorian Andes (Figure 5), whilst shifts toward C4 OM deposition could explain the positive correlation between $\Delta^{14}\text{C-DOC}$ and $\delta^{13}\text{C-DOC}$ observed in glacier outflows. Atmospheric deposition of OM to glaciers, including pollen, is known to be spatially heterogeneous across the supraglacial environment, as well as temporally variable between and within

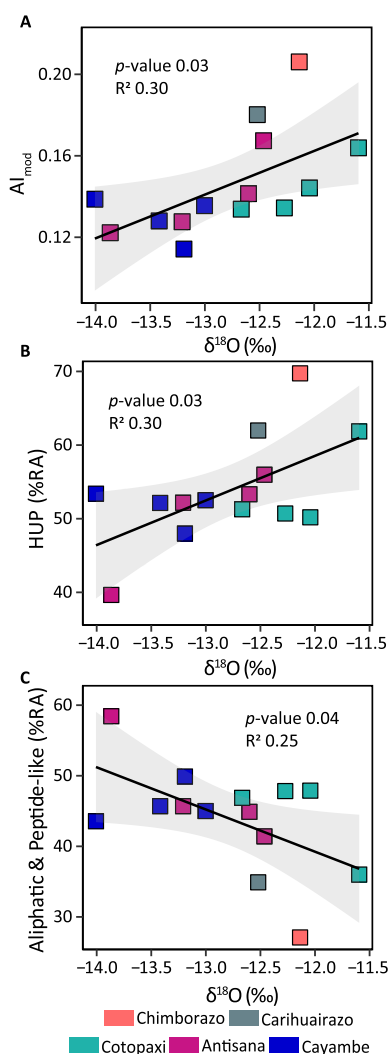


Figure 7. Association between molecular level dissolved organic matter (DOM) composition of glacier outflows and water isotopes ($\delta^{18}\text{O}$). (a) Relative abundance (RA) weighted modified aromaticity index (AI_{mod}). (b and c) the percent RA of highly unsaturated and phenolic (HUP), and aliphatic and peptide-like compounds, respectively. Points are colored according to volcano. Shading represents 95% confidence of regression.

melt seasons (Bourgeois, 2000; Koziol et al., 2019; Reese & Liu., 2005). This may account for some of the variability in isotopic and molecular level signatures seen in this Ecuadorian data set, particularly in supraglacial streams (Tables 1 and 2). Regardless, the exceptionally aliphatic-rich composition of $\Delta^{14}\text{C}$ -DOC enriched glacier streams would indicate that any modern plant-derived material, rich in aromatic and polyphenolic moieties (i.e., those derived directly from plants or pyrogenic alteration), likely has been substantially bio- or photodegraded (Antony et al., 2018; Holt, Kellerman, et al., 2021). More work is required to constrain endmember isotopic compositions relevant to glacier ecosystems, particularly that of atmospheric deposition (including pollen and pyrogenic sources) and microbial biomass. As it stands, a mixture of modern OM from vegetation (C3 and C4) or microbes likely explained the positive correlation between $\Delta^{14}\text{C}$ -DOC and %RA of aliphatic compounds observed in supraglacial and outflow streams, together with the $\delta^{13}\text{C}$ -DOC isotopic heterogeneity of supraglacial DOC (Tables 1 and 2; Figures 3 and 5).

Despite the increase in aliphatic and peptide-like content with $\Delta^{14}\text{C}$ -DOC enrichment, all supraglacial and outflow streams contained a substantial portion (combined $\geq 27\%$ RA) of these compounds regardless of age (Table 2 and Figure 5). Thus, although ancient OM sources to these glacier ecosystems likely had higher aromaticity (i.e., AI_{mod}) than near-modern to modern sources, they were still likely to have been relatively aliphatic-rich. Ancient, aliphatic, and peptide-like compounds in $\Delta^{14}\text{C}$ -DOC deplete supraglacial and outflow streams may have been derived from fossil fuel combustion byproducts ($\Delta^{14}\text{C}$ -DOC $-1,000\text{‰}$, $\delta^{13}\text{C}$ -DOC -35 to -15‰ ; Wang et al., 2022). This OM is likely to have undergone extensive bio- or photodegradation in transport to, or on the glacier surface, as has been suggested for other glacierized regions (e.g., Antony et al., 2018; Holt, Kellerman, et al., 2021; Spencer, Guo, et al., 2014; Stubbins et al., 2012). The small fraction of condensed aromatic and polyphenolics observed across the glacier streams could also be derived from fossil fuel combustion byproducts (Table 2). Similarly, proglacial soils deposited on to the glacier surface ($\Delta^{14}\text{C}$ -DOC $-1,000$ to -291‰ , $\delta^{13}\text{C}$ -DOC -35 to -17‰) or subglacial OM could contribute aged carbon to the glacier DOM pool (Hood et al., 2009; Khedim et al., 2021; Singer et al., 2012; Vinšová et al., 2022). Limited data exists on the concentrations and deposition of anthropogenic derived aerosols on tropical Andean glaciers (Vuille et al., 2018). However, atmospheric deposition of microplastics has been noted on Antisana (proximate to sample sites AN1S1, AN1S2, and AN1-4; Cabrera et al., 2022). Additionally, a large fraction of mercury concentrations ($\sim 40\%$) in high altitude lake sediments (Cajas National Park, southwest Ecuador) are believed to be from atmospheric deposition, and a component of which is likely derived from fossil fuel combustion (Schneider et al., 2021). As such, anthropogenic aerosols are likely to reach the surface of Ecuadorian glaciers via long range atmospheric transport, and may have contributed aged, aliphatic compounds to supraglacial and outflow stream DOM composition.

4.2. Age Offset Between Supraglacial and Outflow Streams

Supraglacial streams were consistently enriched in $\Delta^{14}\text{C}$ -DOC compared to glacier outflows (Tables 1 and 2 and Figures 3–5). Aging of surface DOM compounds has been suggested to occur in situ, via glacier ice formation and subsequent melt (Stubbins et al., 2012), and thus may contribute to the $\Delta^{14}\text{C}$ -DOC offset between supraglacial and outflow streams. However, in these Ecuadorian catchments the residence time of glacier ice is likely short (< 150 years), given the fast ice velocities (e.g., in 2000, Antisana 15 α /AN3's ice flow rate at 5,000 m was $30 \pm 4.9 \text{ ma}^{-1}$; Basantes-Serrano et al., 2016) and small catchment sizes (length < 3 km). Fittingly, available

ice core data extending to the bedrock, from the summit of Chimborazo, covers only the last 120 years, further suggesting most glacier ice was formed within the last two centuries (Vimeux et al., 2009). Thus, given the magnitude of difference in age between supraglacial and outflow stream DOC (mean difference in $\Delta^{14}\text{C-DOC} = -133.9\text{‰}$), melting of 20th century ice could not solely explain this offset.

Instead, integration of aged supraglacial OM from across the supraglacial environment could explain the apparent aging of DOC observed between measured supraglacial streams and their respective outflows. The supraglacial ecosystem is known to be heterogeneous, with a wide range of surface types, gradients, elevations and habitats (e.g., snow, cryoconite holes, clean ice, ice with impurities, supraglacial streams; Hodson et al., 2008). Concentrations of DOC and DOM composition are shown to differ across the supraglacial ecosystems of a glacier (Bhatia et al., 2013; Holland et al., 2019; Musilova et al., 2017; Smith, Diesler, et al., 2018). Specifically, in these Ecuadorian catchments, $\delta^{13}\text{C}$ and $\Delta^{14}\text{C-DOC}$ signatures differed up to 3.8 and 40.9‰, respectively, between supraglacial streams on the same glacier (<200 m from each other). Similarly, the RA of aliphatic and peptide-like compounds ranged up to 9.8% over similar distances (Tables 1 and 2). This may have been in part due to variability across the glacier surface in microbial community composition (Smith, Diesler, et al., 2018), together with variable rates of microbial production (Musilova et al., 2017; Nicholes et al., 2019) and atmospheric deposition (Fellman, Hood, Raymond, Stubbins, & Spencer, 2015; Koziol et al., 2019). Given the small number of supraglacial streams sampled per glacier ($n \leq 2$) in this study, their proximity and compositional range, it is unlikely that the diversity of isotopic and molecular level signatures were completely captured. As such, it is possible that older DOC exists on the glacier surface, which was not measured here (Stubbins et al., 2012). However, higher spatial resolution studies of the supraglacial environment would be required to robustly elucidate this source.

An additional explanation for the $\Delta^{14}\text{C-DOC}$ depletion in Ecuadorian outflows is that subglacial paleosol OM may have also contributed aged DOC to streamwater (Figure 5; Bhatia et al., 2010, 2013; Hood et al., 2009; Kellerman et al., 2020), since outflow DOM is likely an integrated signature of DOM from both supraglacial and subglacial sources. Recently deglaciated soils are a useful proxy for subglacial OM, yet their composition and age are poorly constrained for Ecuadorian glacier catchments (cf., Khedim et al., 2021). It is unclear whether soils or vegetation have ever established above the current glacier extents in Ecuador, given the high altitude, steep gradients, and volcanism. Nonetheless, Antisana soil organic carbon stocks that have formed <20 years since deglaciation contain $\sim 0.6 \text{ g C kg}^{-1}$, within the range of other glacierized settings ($0.12\text{--}14 \text{ g C kg}^{-1}$; Khedim et al., 2021; Vinšová et al., 2022). Typically, deglaciated soil OM is relatively stable, and its associated DOM is rich in condensed aromatic and polyphenolic moieties (>20%RA; Holt, Kellerman, et al., 2021; Khedim et al., 2021; Vinšová et al., 2022). Thus, incorporation of subglacial paleosol DOM would likely result in a shift in outflow DOM composition toward increased aromaticity. This has been proposed to occur in high-latitude catchments, particularly during inefficient drainage periods when basal meltwaters are a significant portion of streamflow and in contact with subglacial OM for prolonged periods (Kellerman et al., 2020). Nonetheless, drainage was likely relatively efficient in Ecuador (due to year-round melt) and supraglacial and outflow DOM was compositionally alike at the molecular level. Furthermore, typically aromaticity and %RA HUP formulae declined in outflow samples compared to their respective supraglacial streams (Table 1 and Figures 3 and 5). Thus, leaching of subglacial soils was unlikely to explain the age offset observed between supraglacial and outflow streams.

However, subglacial paleosol organic carbon may also sustain subglacial microbial communities and thus may have been substantially biodegraded (Bhatia et al., 2013; Vinšová et al., 2022). Microbial metabolism of subglacial OM could supply aged aliphatic-rich DOM to streamwater as it is routed through the glacier hydrological system, explaining the age offset seen between supraglacial and outflow streams. Similarly, chemolithoautotrophic subglacial microbes may have fixed aged dissolved inorganic carbon (DIC) produced from the respiration of subglacial OM (Boyd et al., 2014). However, subglacial microbial processes would be a surprising source at these Ecuadorian sites, since subglacial microbial processes are sustained by subglacial paleosol material. As such, we would expect a shift toward increased aromaticity caused by leaching of this substrate alongside the microbially fixed or processed DOM. However, such a shift toward increased aromaticity was not observed. Similarly, alternative sources of aged DIC to Ecuadorian catchments were unclear, since the bedrock lacks carbonate bearing minerals (i.e., geology is primarily volcanic igneous rock; andesitic/basaltic) and residence times of trapped solutes were likely shorter than the age offset between supraglacial and outflow $\Delta^{14}\text{C-DOC}$. As such, the possibility for subglacial chemolithotrophy is unclear. Subglacial sources of microbial DOM are enigmatic and evidence to support their presence is limited in this data set; nevertheless, they cannot completely be excluded as a source of aged, aliphatic-rich DOM to Ecuadorian outflow streams.

4.3. Regional Drivers of Glacier Outflow DOM Composition

The relationship between molecular level DOM composition and $\delta^{18}\text{O}$ suggested precipitation gradients across the Ecuadorian Andes may partly control glacier outflow DOM composition (Figures 6 and 7), likely due to changing quality and quantity of atmospherically deposited OM. Precipitation across the northern Ecuadorian Andes is highly complex and derived from air masses of both Pacific and Atlantic origin. Both have enriched $\delta^{18}\text{O}$ signatures (annual average $\sim 5\%$), the latter due to intensive recycling of moisture over the Amazon, resulting in enrichment despite the vast distance ($>2,000$ km) from the Atlantic coast (Garcia et al., 1998). The $\delta^{18}\text{O}$ signatures of precipitation across the northern Ecuadorian Andes are highly variable, both interannually and seasonally. At $0\text{--}5^\circ\text{S}$ (period 1976–1999, $>2,400$ m), observed and modeled seasonal shifts in $\delta^{18}\text{O}$ have been shown to be between 8 and 10‰, and yearly precipitation-weighted mean $\delta^{18}\text{O}$ values have a 4‰ interannual range (Garcia et al., 1998; Insel et al., 2013). Given the overlap in $\delta^{18}\text{O}$ signatures between precipitation of Pacific and Amazonian origin, variability in $\delta^{18}\text{O}$ of precipitation over the northern Andes, and that glacial outflow streamflow is likely a mixture of recent precipitation, snowmelt, and surface ice melt, it is not possible to quantitatively partition the $\delta^{18}\text{O}$ of streamwater into Amazonian and Pacific influence for each volcano. Hence, it is unclear which air mass was driving the south to north depletion in glacier outflow $\delta^{18}\text{O}$ (Figure 2). Nonetheless, two scenarios may help explain trends between molecular level DOM composition and streamwater $\delta^{18}\text{O}$ of glacier outflows across Ecuador (Figure 7).

First, air masses of Atlantic and Pacific origin may carry OM of different quality and quantity to the glacier surface. As such, across the region, Pacific and Atlantic air masses may influence the water isotope and DOM composition of precipitation by different magnitudes. Thus, variability in the origins of precipitation may translate to differences in glacier outflow DOM composition. Seasonal variability in glacier ice $\delta^{18}\text{O}$ is shown to result from changing prominence of precipitation of Pacific and Amazonian origin, where marine and biomass burning biomarkers covary with these shifts (Ginot et al., 2002). Namely, increased precipitation of Pacific origin coincides with an increase in marine tracers and a decrease in vegetation tracers (Ginot et al., 2002). Thus, increased inputs of Amazonian precipitation may result in $\delta^{18}\text{O}$ depletion concomitant with an increased deposition of bio- or photodegraded, modern, burnt biomass to the glacier surface, explaining the increased %RA of aliphatic compounds with enrichment in $\Delta^{14}\text{C}\text{-DOC}$, seen here toward the north of the region (Figures 5 and 6). To accurately assign these influences, future studies must place constraints on $\delta^{18}\text{O}$ and DOM composition of Amazonian and Pacific derived precipitation.

Second, $\delta^{18}\text{O}$ depletion in the northern catchments could also reflect greater distances Pacific storms track to reach the glaciers, where Pacific sources of OM maybe rained out along a storm trajectory. As a result, with greater distances a declining portion of DOC may be derived from atmospheric deposition (e.g., marine and fossil combustion byproduct OM). The rainout of DOC along storm trajectories has been shown to occur across the surface of the Juneau icefield, Alaska, where DOC concentrations decline toward the interior (Fellman, Hood, Raymond, Stubbins, & Spencer, 2015). Unlike large glaciers and ice sheets, where there are fewer local allochthonous inputs toward the interior, Ecuadorian catchments are proximate to proglacial soil and vegetation (Fellman, Hood, Raymond, Stubbins, & Spencer, 2015; Stibal et al., 2012). This material could be blown on to the glacier surface contributing OM or seeding supraglacial microbial processes. As such, in Ecuadorian catchments further along Pacific storm trajectories, local wind-blown allochthonous sources (e.g., plant material and pollen) and in situ microbial production on the ice surface may be the dominant DOM source to glacier outflow streams. This may result in $\Delta^{14}\text{C}\text{-DOC}$ and aliphatic enriched DOM, alongside streamwater $\delta^{18}\text{O}$ depletion. Moreover, these DOM signatures may be masked in catchments that receive greater inputs of aged atmospheric carbon. The correlations between $\delta^{18}\text{O}$ and DOM composition were in all likelihood explained by a combination of both scenarios, and hence represented a mixed signal of a rainout effect along Pacific storm tracks, combined with a changing dominance of air masses of Pacific and Amazonian origin across the region.

Despite uncertainty in the cause of regional gradients in water isotopic composition, these results underscore that atmospheric deposition, its quality and thus origins, may partly drive regional variability in DOM composition across Ecuadorian glacier catchments. More research should be directed toward constraining the origin of atmospherically deposited OM to glacier surfaces, since this may influence the age and quality of DOM exported from glaciers to downstream ecosystems, with potentially different implications for the carbon cycle. For improved understanding of how glacier ecosystems will change with globally unabated retreat, it is apparent from this study, specifically the stark offset in $\Delta^{14}\text{C}\text{-DOC}$ between supraglacial and outflow streamwater and regional

gradients in DOM composition across Ecuador, that future work must address variability in supraglacial and outflow DOM composition and source. This requires an improved knowledge of the origin of atmospherically deposited and subglacial OM matter sources, as well as higher spatiotemporal resolution studies of DOM variability across glacier surfaces.

Global Research Collaboration Statement

We thank Pontificia Universidad Católica del Ecuador for their partnership, support and use of resources during the field campaign. Freddy Ramirez is thanked for his local insight, guiding, and assistance in the collection of glacier samples. We thank all the mountain guides and refuge staff for their hospitality and for accommodating our research. Fieldwork was conducted under the global research permit of Escuela Politécnica Nacional from the Minister del Ambiente, Direction National de Biodiversidad.

Data Availability Statement

Raw FT-ICR MS spectra files and associated elemental compositions are publicly available through the Open Science Framework (OSF; <https://osf.io/xtf4a/>) and can be accessed using the following <https://doi.org/10.17605/OSF.IO/XTF4A>.

Acknowledgments

Seneca Randolph and Sophia Gomez at Florida State University are thanked for help with sample preparation for DOC analysis. Dr. Vennemann (University of Lausanne) and NOSAMS are thanked for water and carbon isotopic analysis, respectively. A portion of this work was funded by the Vanishing Glaciers Project from the NOMIS foundation. FT-ICR MS analysis was performed in the Ion Cyclotron Resonance User Facility at the National High Magnetic Field Laboratory, which is supported by the National Science Foundation Division of Chemistry and Division of Materials Research through DMR 16-44779, and the State of Florida. E.H. was supported by an award to Alaska EPSCoR from the National Science Foundation (OIA 1757348).

References

- Aiken, G. R., Spencer, R. G. M., Striegl, R. G., Schuster, P. F., & Raymond, P. A. (2014). Influences of glacier melt and permafrost thaw on the age of dissolved organic carbon in the Yukon River basin. *Global Biogeochemical Cycles*, 28(5), 525–537. <https://doi.org/10.1002/2013gb004764>
- Andrews, M. G., Jacobson, A. D., Osburn, M. R., & Flynn, T. M. (2018). Dissolved carbon dynamics in meltwaters from the Russell glacier, Greenland ice sheet. *Journal of Geophysical Research: Biogeosciences*, 123(9), 2922–2940. <https://doi.org/10.1029/2018jg004458>
- Antony, R., Willoughby, A. S., Grannas, A. M., Catanzano, V., Sleighter, R. L., Thamban, M., & Hatcher, P. G. (2018). Photo-biochemical transformation of dissolved organic matter on the surface of the coastal East Antarctic ice sheet. *Biogeochemistry*, 141(2), 229–247. <https://doi.org/10.1007/s10533-018-0516-0>
- Arimitsu, M. L., Hobson, K. A., Webber, D. A. N., Piatt, J. F., Hood, E. W., & Fellman, J. B. (2018). Tracing biogeochemical subsidies from glacier runoff into Alaska's coastal marine food webs. *Global Change Biology*, 24(1), 387–398. <https://doi.org/10.1111/gcb.13875>
- Barta, B., Mouillet, C., Espinosa, R., Andino, P., Jacobsen, D., & Christoffersen, K. S. (2018). Glacial-fed and páramo lake ecosystems in the tropical high Andes. *Hydrobiologia*, 813(1), 19–32. <https://doi.org/10.1007/s10750-017-3428-4>
- Basantes-Serrano, R., Rabatel, A., Francou, B., Vincent, C., Maisincho, L., Cáceres, B., et al. (2016). Slight mass loss revealed by reanalyzing glacier mass-balance observations on Glaciar Antisana 15α (inner tropics) during the 1995–2012 period. *Journal of Glaciology*, 62(231), 124–136. <https://doi.org/10.1017/jog.2016.17>
- Behnke, M. I., McClelland, J. W., Tank, S. E., Kellerman, A. M., Holmes, R. M., Haghpor, N., et al. (2021). Pan-Arctic riverine dissolved organic matter: Synchronous molecular stability, shifting sources and subsidies. *Global Biogeochemical Cycles*, 35(4), e2020GB006871. <https://doi.org/10.1029/2020gb006871>
- Behnke, M. I., Stubbins, A., Fellman, J. B., Hood, E., Dittmar, T., & Spencer, R. G. (2020). Dissolved organic matter sources in glacierized watersheds delineated through compositional and carbon isotopic modeling. *Limnology & Oceanography*, 66(2), 438–451. <https://doi.org/10.1002/lno.11615>
- Benn, D., & Evans, D. J. (2014). *Glaciers and glaciation*. Routledge.
- Bhatia, M. P., Das, S. B., Longnecker, K., Charette, M. A., & Kujawinski, E. B. (2010). Molecular characterization of dissolved organic matter associated with the Greenland ice sheet. *Geochimica et Cosmochimica Acta*, 74(13), 3768–3784. <https://doi.org/10.1016/j.gca.2010.03.035>
- Bhatia, M. P., Das, S. B., Xu, L., Charette, M. A., Wadham, J. L., & Kujawinski, E. B. (2013). Organic carbon export from the Greenland ice sheet. *Geochimica et Cosmochimica Acta*, 109, 329–344. <https://doi.org/10.1016/j.gca.2013.02.006>
- Blakney, G. T., Hendrickson, C. L., & Marshall, A. G. (2011). Predator data station: A fast data acquisition system for advanced FT-ICR MS experiments. *International Journal of Mass Spectrometry*, 306(2–3), 246–252. <https://doi.org/10.1016/j.ijms.2011.03.009>
- Boom, A., Mora, G., Cleef, A., & Hooghiemstra, H. (2001). High altitude C4 grasslands in the northern Andes: Relicts from glacial conditions? *Review of Palaeobotany and Palynology*, 115(3–4), 147–160. [https://doi.org/10.1016/s0034-6667\(01\)00056-2](https://doi.org/10.1016/s0034-6667(01)00056-2)
- Bourgeois, J. C. (2000). Seasonal and interannual pollen variability in snow layers of arctic ice caps. *Review of Palaeobotany and Palynology*, 108(1–2), 17–36. [https://doi.org/10.1016/s0034-6667\(99\)00031-7](https://doi.org/10.1016/s0034-6667(99)00031-7)
- Boyd, E. S., Hamilton, T. L., Havig, J. R., Skidmore, M. L., & Shock, E. L. (2014). Chemolithotrophic primary production in a subglacial ecosystem. *Applied and Environmental Microbiology*, 80(19), 6146–6153. <https://doi.org/10.1128/aem.01956-14>
- Buytaert, W., Céleri, R., De Bièvre, B., Cisneros, F., Wyseure, G., Deckers, J., & Hofstede, R. (2006). Human impact on the hydrology of the Andean páramos. *Earth-Science Reviews*, 79(1–2), 53–72. <https://doi.org/10.1016/j.earscirev.2006.06.002>
- Buytaert, W., Cuesta-Camacho, F., & Tobón, C. (2011). Potential impacts of climate change on the environmental services of humid tropical alpine regions. *Global Ecology and Biogeography*, 20(1), 19–33. <https://doi.org/10.1111/j.1466-8238.2010.00585.x>
- Cabrera, M., Moulatlet, G. M., Valencia, B. G., Maisincho, L., Rodríguez-Barroso, R., Albendín, G., et al. (2022). Microplastics in a tropical Andean glacier: A transportation process across the Amazon Basin? *Science of the Total Environment*, 805, 150334. <https://doi.org/10.1016/j.scitotenv.2021.150334>
- Cauvy-Fraunié, S., Condom, T., Rabatel, A., Villacis, M., Jacobsen, D., & Dangles, O. (2013). Glacial influence in tropical mountain hydrosystems evidenced by the diurnal cycle in water levels. *Hydrology and Earth System Sciences*, 17(12), 4803–4816. <https://doi.org/10.5194/hess-17-4803-2013>

- Cerling, T. E., Harris, J. M., MacFadden, B. J., Leakey, M. G., Quade, J., Eisenmann, V., & Ehleringer, J. R. (1997). Global vegetation change through the Miocene/Pliocene boundary. *Nature*, *389*(6647), 153–158. <https://doi.org/10.1038/38229>
- Chen, Y., Morton, D. C., Jin, Y., Collatz, G. J., Kasibhatla, P. S., van der Werf, G. R., et al. (2013). Long-term trends and interannual variability of forest, savanna and agricultural fires in South America. *Carbon Management*, *4*(6), 617–638. <https://doi.org/10.4155/cmt.13.61>
- Corilo, Y. (2014). *PetroOrg software*. Florida State University. All rights reserved.
- Csank, A. Z., Czimczik, C. I., Xu, X., & Welker, J. M. (2019). Seasonal patterns of riverine carbon sources and export in NW Greenland. *Journal of Geophysical Research: Biogeosciences*, *124*(4), 840–856. <https://doi.org/10.1029/2018jg004895>
- Dittmar, T., Koch, B., Hertkorn, N., & Kattner, G. (2008). A simple and efficient method for the solid-phase extraction of dissolved organic matter (SPE-DOM) from seawater. *Limnology and Oceanography: Methods*, *6*(6), 230–235. <https://doi.org/10.4319/lom.2008.6.230>
- Dubnick, A., Wadham, J., Tranter, M., Sharp, M., Orwin, J., Barker, J., et al. (2017). Trickle or treat: The dynamics of nutrient export from polar glaciers. *Hydrological Processes*, *31*(9), 1776–1789. <https://doi.org/10.1002/hyp.11149>
- Favier, V., Wagnon, P., & Ribstein, P. (2004). Glaciers of the outer and inner tropics: A different behaviour but a common response to climatic forcing. *Geophysical Research Letters*, *31*(16), L16403. <https://doi.org/10.1029/2004gl020654>
- Fegel, T., Boot, C. M., Broeckling, C. D., Baron, J. S., & Hall, E. K. (2019). Assessing the chemistry and bioavailability of dissolved organic matter from glaciers and rock glaciers. *Journal of Geophysical Research: Biogeosciences*, *124*(7), 1988–2004. <https://doi.org/10.1029/2018jg004874>
- Fellman, J. B., D'Amore, D. V., Hood, E., & Boone, R. D. (2008). Fluorescence characteristics and biodegradability of dissolved organic matter in forest and wetland soils from coastal temperate watersheds in southeast Alaska. *Biogeochemistry*, *88*(2), 169–184. <https://doi.org/10.1007/s10533-008-9203-x>
- Fellman, J. B., Hood, E., Raymond, P. A., Hudson, J., Bozeman, M., & Arimitsu, M. (2015). Evidence for the assimilation of ancient glacier organic carbon in a proglacial stream food web. *Limnology & Oceanography*, *60*(4), 1118–1128. <https://doi.org/10.1002/lno.10088>
- Fellman, J. B., Hood, E., Raymond, P. A., Stubbins, A., & Spencer, R. G. M. (2015). Spatial variation in the origin of dissolved organic carbon in snow on the Juneau icefield, Southeast Alaska. *Environmental Science & Technology*, *49*(19), 11492–11499. <https://doi.org/10.1021/acs.est.5b02685>
- Fellman, J. B., Hood, E., Spencer, R. G., Stubbins, A., & Raymond, P. A. (2014). Watershed glacier coverage influences dissolved organic matter biogeochemistry in coastal watersheds of southeast Alaska. *Ecosystems*, *17*(6), 1014–1025. <https://doi.org/10.1007/s10021-014-9777-1>
- Fellman, J. B., Spencer, R. G., Hernes, P. J., Edwards, R. T., D'Amore, D. V., & Hood, E. (2010). The impact of glacier runoff on the biodegradability and biochemical composition of terrigenous dissolved organic matter in near-shore marine ecosystems. *Marine Chemistry*, *121*(1–4), 112–122. <https://doi.org/10.1016/j.marchem.2010.03.009>
- Feng, L., Xu, J., Kang, S., Li, X., Li, Y., Jiang, B., & Shi, Q. (2016). Chemical composition of microbe-derived dissolved organic matter in cryoconite in Tibetan Plateau glaciers: Insights from Fourier transform ion cyclotron resonance mass spectrometry analysis. *Environmental Science & Technology*, *50*(24), 13215–13223. <https://doi.org/10.1021/acs.est.6b03971>
- Garcia, M., Villalba, F., Araguas-Araguas, L., & Rozanski, K. (1998). The role of atmospheric circulation patterns in controlling the regional distribution of stable isotope contents in precipitation: Preliminary results from two transects in the Ecuadorian Andes. In *Isotope techniques in the study of environmental change*.
- Ginot, P., Schwikowski, M., Schotterer, U., Stichler, W., Gäggeler, H. W., Francou, B., et al. (2002). Potential for climate variability reconstruction from Andean glaciochemical records. *Annals of Glaciology*, *35*, 443–450. <https://doi.org/10.3189/172756402781816618>
- Gospodinova, K., McNichol, A., Gagnon, A., & Shah Walter, S. (2016). Rapid extraction of dissolved inorganic carbon from seawater and groundwater samples for radiocarbon dating. *Limnology and Oceanography: Methods*, *14*(1), 24–30. <https://doi.org/10.1002/lom3.10066>
- Griffith, D. R., McNichol, A. P., Xu, L., McLaughlin, F. A., Macdonald, R., Brown, K., & Eglinton, T. I. (2012). Carbon dynamics in the western Arctic ocean: Insights from full-depth carbon isotope profiles of DIC, DOC, and POC. *Biogeosciences*, *9*(3), 1217–1224. <https://doi.org/10.5194/bg-9-1217-2012>
- Gualco, L. F., Maisincho, L., Villacís, M., Campozano, L., Favier, V., Ruiz-Hernández, J.-C., & Condom, T. (2022). Assessing the contribution of glacier melt to discharge in the tropics: The case of study of the Antisana glacier 12 in Ecuador. *Frontiers of Earth Science*, *568*. <https://doi.org/10.3389/feart.2022.732635>
- Hemingway, J. D., Spencer, R. G. M., Podgorski, D. C., Zito, P., Sen, I. S., & Galy, V. V. (2019). Glacier meltwater and monsoon precipitation drive Upper Ganges Basin dissolved organic matter composition. *Geochimica et Cosmochimica Acta*, *244*, 216–228. <https://doi.org/10.1016/j.gca.2018.10.012>
- Hendrickson, C. L., Quinn, J. P., Kaiser, N. K., Smith, D. F., Blakney, G. T., Chen, T., et al. (2015). 21 tesla Fourier transform ion cyclotron resonance mass spectrometer: A national resource for ultrahigh resolution mass analysis. *Journal of the American Society for Mass Spectrometry*, *26*(9), 1626–1632. <https://doi.org/10.1007/s13361-015-1182-2>
- Hertkorn, N., Ruecker, C., Meringer, M., Gugisch, R., Frommberger, M., Perdue, E., et al. (2007). High-precision frequency measurements: Indispensable tools at the core of the molecular-level analysis of complex systems. *Analytical and Bioanalytical Chemistry*, *389*(5), 1311–1327. <https://doi.org/10.1007/s00216-007-1577-4>
- Hobson, K. A., & Welch, H. E. (1992). Determination of trophic relationships within a high Arctic marine food web using $\delta^{13}\text{C}$ and $\delta^{15}\text{N}$ analysis. *Marine Ecology Progress Series*, *84*, 9–18. <https://doi.org/10.3354/meps084009>
- Hodson, A., Anesio, A. M., Tranter, M., Fountain, A., Osborn, M., Priscu, J., et al. (2008). Glacial ecosystems. *Ecological Monographs*, *78*(1), 41–67. <https://doi.org/10.1890/07-0187.1>
- Holding, J. M., Duarte, C. M., Delgado-Huertas, A., Soetaert, K., Vonk, J. E., Agustí, S., et al. (2017). Autochthonous and allochthonous contributions of organic carbon to microbial food webs in Svalbard fjords. *Limnology & Oceanography*, *62*(3), 1307–1323. <https://doi.org/10.1002/lno.10526>
- Holland, A. T., Williamson, C. J., Sgouridis, F., Tedstone, A. J., McCutcheon, J., Cook, J. M., et al. (2019). Dissolved organic nutrients dominate melting surface ice of the Dark Zone (Greenland Ice Sheet). *Biogeosciences*, *16*(16), 3283–3296. <https://doi.org/10.5194/bg-16-3283-2019>
- Holt, A. D., Fellman, J., Hood, E., Kellerman, A. M., Raymond, P., Stubbins, A., et al. (2021). The evolution of stream dissolved organic matter composition following glacier retreat in coastal watersheds of southeast Alaska. *Biogeochemistry*, 1–18. <https://doi.org/10.1007/s10533-021-00815-6>
- Holt, A. D., Kellerman, A. M., Li, W., Stubbins, A., Wagner, S., McKenna, A., et al. (2021). Assessing the role of photochemistry in driving the composition of dissolved organic matter in glacier runoff. *Journal of Geophysical Research: Biogeosciences*, *126*(12), e2021JG006516. <https://doi.org/10.1029/2021jg006516>
- Hood, E., Battin, T., Fellman, J., O'Neel, S., & Spencer, R. (2015). Storage and release of organic carbon from glaciers and ice sheets. *Nature Geoscience*, *8*(2), 91–96. <https://doi.org/10.1038/ngeo2331>
- Hood, E., Fellman, J., Spencer, R., Hernes, P., Edwards, R., D'Amore, D., & Scott, D. (2009). Glaciers as a source of ancient and labile organic matter to the marine environment. *Letters to Nature*, *462*(24), 1044–1048. <https://doi.org/10.1038/nature08580>

- Insel, N., Poulsen, C. J., Sturm, C., & Ehlers, T. A. (2013). Climate controls on Andean precipitation $\delta^{18}\text{O}$ interannual variability. *Journal of Geophysical Research: Atmospheres*, *118*(17), 9721–9742. <https://doi.org/10.1002/jgrd.50619>
- Kellerman, A., Hawkings, J., Wadham, J., Kohler, T., Stibal, M., Grater, E., et al. (2020). Glacier outflow dissolved organic matter as a window into seasonally changing carbon sources: Leverett Glacier, Greenland. *Journal of Geophysical Research: Biogeosciences*, *125*(4), e2019JG005161. <https://doi.org/10.1029/2019jg005161>
- Kellerman, A. M., Vonk, J., McColough, S., Podgorski, D. C., van Winden, E., Hawkings, J. R., et al. (2021). Molecular signatures of glacial dissolved organic matter from Svalbard and Greenland. *Global Biogeochemical Cycles*, *35*(3), e2020GB006709. <https://doi.org/10.1029/2020gb006709>
- Khedim, N., Cecillon, L., Poulencard, J., Barré, P., Baudin, F., Marta, S., et al. (2021). Topsoil organic matter build-up in glacier forelands around the world. *Global Change Biology*, *27*(8), 1662–1677. <https://doi.org/10.1111/gcb.15496>
- Koch, B., & Dittmar, T. (2006). From mass to structure: An aromaticity index for high-resolution mass data of natural organic matter. *Rapid Communications in Mass Spectrometry*, *20*(5), 926–932. <https://doi.org/10.1002/rcm.2386>
- Koch, B., & Dittmar, T. (2016). From mass to structure: An aromaticity index for high-resolution mass data of natural organic matter. *Rapid Communications in Mass Spectrometry*, *30*(1), 250. <https://doi.org/10.1002/rcm.7433>
- Koch, D., & Hansen, J. (2005). Distant origins of arctic black carbon: A Goddard Institute for space studies ModelE experiment. *Journal of Geophysical Research*, *110*(D4), D04204. <https://doi.org/10.1029/2004jd005296>
- Kohn, M. J. (2010). Carbon isotope compositions of terrestrial C3 plants as indicators of (paleo) ecology and (paleo) climate. *Proceedings of the National Academy of Sciences of the United States of America*, *107*(46), 19691–19695. <https://doi.org/10.1073/pnas.1004933107>
- Koziol, K. A., Moggridge, H. L., Cook, J. M., & Hodson, A. J. (2019). Organic carbon fluxes of a glacier surface: A case study of Foxfonna, a small Arctic glacier. *Earth Surface Processes and Landforms*, *44*(2), 405–416. <https://doi.org/10.1002/esp.4501>
- Kurek, M. R., Stubbins, A., Drake, T. W., Dittmar, T., MS Moura, J., Holmes, R. M., et al. (2022). Organic molecular signatures of the Congo river and comparison to the Amazon. *Global Biogeochemical Cycles*, *36*(6), e2022GB007301. <https://doi.org/10.1029/2022gb007301>
- LaRowe, D. E., & Van Cappellen, P. (2011). Degradation of natural organic matter: A thermodynamic analysis. *Geochimica et Cosmochimica Acta*, *75*(8), 2030–2042. <https://doi.org/10.1016/j.gca.2011.01.020>
- Lawson, E. C., Bhatia, M. P., Wadham, J. L., & Kujawinski, E. B. (2014). Continuous summer export of nitrogen-rich organic matter from the Greenland Ice Sheet inferred by ultrahigh resolution mass spectrometry. *Environmental Science & Technology*, *48*(24), 14248–14257. <https://doi.org/10.1021/es501732h>
- Lê, S., Josse, J., & Husson, F. (2008). FactoMineR: An R package for Multivariate analysis. *Journal of Statistical Software*, *25*(1). <https://doi.org/10.18637/jss.v025.i01>
- Ledru, M.-P., Jomelli, V., Samaniego, P., Vuille, M., Hidalgo, S., Herrera, M., & Ceron, C. (2013). The Medieval climate anomaly and the Little ice age in the eastern Ecuadorian Andes. *Climate of the Past*, *9*(1), 307–321. <https://doi.org/10.5194/cp-9-307-2013>
- Magalhães, N. d., Evangelista, H., Condom, T., Rabatel, A., & Ginot, P. (2019). Amazonian biomass burning enhances tropical Andean glaciers melting. *Scientific Reports*, *9*(1), 1–12. <https://doi.org/10.1038/s41598-019-53284-1>
- McMahon, K. W., Ambrose, W. G., Jr., Johnson, B. J., Sun, M.-Y., Lopez, G. R., Clough, L. M., & Carroll, M. L. (2006). Benthic community response to ice algae and phytoplankton in Ny Ålesund, Svalbard. *Marine Ecology Progress Series*, *310*, 1–14. <https://doi.org/10.3354/meps310001>
- Mladenov, N., Sommaruga, R., Morales-Baquero, R., Laurion, I., Camarero, L., Diéguez, M. C., et al. (2011). Dust inputs and bacteria influence dissolved organic matter in clear alpine lakes. *Nature Communications*, *2*(1), 1–7. <https://doi.org/10.1038/ncomms1411>
- Musilova, M., Tranter, M., Wadham, J., Telling, J., Tedstone, A., & Anesio, A. M. (2017). Microbially driven export of labile organic carbon from the Greenland ice sheet. *Nature Geoscience*, *10*(5), 360–365. <https://doi.org/10.1038/ngeo2920>
- Nicholes, M. J., Williamson, C. J., Tranter, M., Holland, A., Poniecka, E., Yallop, M. L., et al. (2019). Bacterial dynamics in supraglacial habitats of the Greenland ice sheet. *Frontiers in Microbiology*, *10*, 1366. <https://doi.org/10.3389/fmicb.2019.01366>
- Powell, R. L., & Still, C. J. (2009). Biogeography of C3 and C4 vegetation in south America. *XIV Simpósio Brasileiro Sensoriamento Remoto*, *14*, 2935–2942.
- Rabatel, A., Francou, B., Soruco, A., Gomez, J., Cáceres, B., Ceballos, J. L., et al. (2013). Current state of glaciers in the tropical Andes: A multi-century perspective on glacier evolution and climate change. *The Cryosphere*, *7*(1), 81–102. <https://doi.org/10.5194/tc-7-81-2013>
- R Core Team. (2020). *R: A language and environment for statistical computing*. R Foundation for Statistical Computing.
- Reese, C. A., & Liu, K. (2005). Interannual variability in pollen dispersal and deposition on the tropical Quelccaya Ice Cap. *The Professional Geographer*, *57*(2), 185–197. <https://doi.org/10.1111/j.0033-0124.2005.00471.x>
- Riedel, T., Biester, H., & Dittmar, T. (2012). Molecular fractionation of dissolved organic matter with metal salts. *Environmental Science & Technology*, *46*(8), 4419–4426. <https://doi.org/10.1021/es203901u>
- Roberts, M. L., Burton, J. R., Elder, K. L., Longworth, B. E., McIntyre, C. P., von Reden, K. F., et al. (2010). A high-performance ^{14}C accelerator mass spectrometry system. *Radiocarbon*, *52*(2), 228–235. <https://doi.org/10.1017/s003822200045252>
- Savory, J. J., Kaiser, N. K., McKenna, A. M., Xian, F., Blakney, G. T., Rodgers, R. P., et al. (2011). Parts-per-billion Fourier transform ion cyclotron resonance mass measurement accuracy with a “walking” calibration equation. *Analytical Chemistry*, *83*(5), 1732–1736. Retrieved from <https://pubs.acs.org/doi/10.1021/ac102943z>
- Schneider, T., Musa Bandowe, B. A., Bigalke, M., Mestrot, A., Hampel, H., Mosquera, P. V., et al. (2021). 250-year records of mercury and trace element deposition in two lakes from Cajas National Park, SW Ecuadorian Andes. *Environmental Science & Pollution Research*, *28*(13), 16227–16243. <https://doi.org/10.1007/s11356-020-11437-0>
- Singer, G. A., Fasching, C., Wilhelm, L., Niggemann, J., Steier, P., Dittmar, T., & Battin, T. J. (2012). Biogeochemically diverse organic matter in Alpine glaciers and its downstream fate. *Nature Geoscience*, *5*(10), 710–714. <https://doi.org/10.1038/ngeo1581>
- Smith, D. F., Podgorski, D. C., Rodgers, R. P., Blakney, G. T., & Hendrickson, C. L. (2018). 21 tesla FT-ICR mass spectrometer for ultrahigh-resolution analysis of complex organic mixtures. *Analytical Chemistry*, *90*(3), 2041–2047. <https://doi.org/10.1021/acs.analchem.7b04159>
- Smith, H. J., Diesler, M., McKnight, D. M., SanClements, M., & Foreman, C. M. (2018). Relationship between dissolved organic matter quality and microbial community composition across polar glacial environments. *FEMS Microbiology Ecology*, *94*(7), fiy090. <https://doi.org/10.1093/femsec/fiy090>
- Spencer, R. G., Guo, W., Raymond, P. A., Dittmar, T., Hood, E., Fellman, J., & Stubbins, A. (2014). Source and biolability of ancient dissolved organic matter in glacier and lake ecosystems on the Tibetan Plateau. *Geochimica et Cosmochimica Acta*, *142*, 64–74. <https://doi.org/10.1016/j.gca.2014.08.006>
- Spencer, R. G. M., Vermilyea, A., Fellman, J., Raymond, P., Stubbins, A., Scott, D., & Hood, E. (2014). Seasonal variability of organic matter composition in an Alaskan glacier outflow: Insights into glacier carbon sources. *Environmental Research Letters*, *9*(5), 55005. <https://doi.org/10.1088/1748-9326/9/5/055005>

- Stibal, M., Šabacká, M., & Žárský, J. (2012). Biological processes on glacier and ice sheet surfaces. *Nature Geoscience*, 5(11), 771–774. <https://doi.org/10.1038/ngeo1611>
- Stubbins, A., Hood, E., Raymond, P. A., Aiken, G. R., Sleighter, R. L., Hernes, P. J., et al. (2012). Anthropogenic aerosols as a source of ancient dissolved organic matter in glaciers. *Nature Geoscience*, 5(3), 198–201. <https://doi.org/10.1038/ngeo1403>
- Textor, S. R., Guillemette, F., Zito, P. A., & Spencer, R. G. M. (2018). An assessment of dissolved organic carbon biodegradability and priming in blackwater systems. *Journal of Geophysical Research: Biogeosciences*, 123(9), 2998–3015. <https://doi.org/10.1029/2018jg004470>
- Vimeux, F., Ginot, P., Schwikowski, M., Vuille, M., Hoffmann, G., Thompson, L. G., & Schotterer, U. (2009). Climate variability during the last 1000 years inferred from Andean ice cores: A review of methodology and recent results. *Palaeogeography, Palaeoclimatology, Palaeoecology*, 281(3–4), 229–241. <https://doi.org/10.1016/j.palaeo.2008.03.054>
- Vinšová, P., Kohler, T., Simpson, M., Hajdas, I., Yde, J., Falteisek, L., et al. (2022). The biogeochemical Legacy of arctic subglacial sediments exposed by glacier retreat. *Global Biogeochemical Cycles*, 36(3), e2021GB007126. <https://doi.org/10.1029/2021gb007126>
- Vuille, M., Carey, M., Huggel, C., Buytaert, W., Rabatel, A., Jacobsen, D., et al. (2018). Rapid decline of snow and ice in the tropical Andes—Impacts, uncertainties and challenges ahead. *Earth-Science Reviews*, 176, 195–213. <https://doi.org/10.1016/j.earscirev.2017.09.019>
- Wang, P., Zhou, W., Xiong, X., Wu, S., Niu, Z., Cheng, P., et al. (2022). Stable carbon isotopic characteristics of fossil fuels in China. *Science of the Total Environment*, 805, 150240. <https://doi.org/10.1016/j.scitotenv.2021.150240>
- Xu, L., Roberts, M. L., Elder, K. L., Hansman, R. L., Gagnon, A. R., & Kurz, M. D. (2022). Radiocarbon in dissolved organic carbon by UV oxidation: An update of procedures and Blank characterization at NOSAMS. *Radiocarbon*, 64, 1–5. <https://doi.org/10.1017/rdc.2022.4>
- Xu, L., Roberts, M. L., Elder, K. L., Kurz, M. D., McNichol, A. P., Reddy, C. M., et al. (2021). Radiocarbon in dissolved organic carbon by UV oxidation: Procedures and Blank characterization at nosams. *Radiocarbon*, 63(1), 357–374. <https://doi.org/10.1017/rdc.2020.102>
- Zemp, M., Huss, M., Thibert, E., Eckert, N., McNabb, R., Huber, J., et al. (2019). Global glacier mass changes and their contributions to sea-level rise from 1961 to 2016. *Nature*, 568(7752), 382–386. <https://doi.org/10.1038/s41586-019-1071-0>
- Zhou, Y., Zhou, L., He, X., Jang, K.-S., Yao, X., Hu, Y., et al. (2019). Variability in dissolved organic matter composition and biolability across gradients of glacial coverage and distance from glacial terminus on the Tibetan Plateau. *Environmental Science & Technology*, 53(21), 12207–12212. <https://doi.org/10.1021/acs.est.9b03348>